

NH-Ade Faisal-etal-2011

by Ade Faisal

Submission date: 20-Nov-2018 09:04PM (UTC+0700)

Submission ID: 1042566488

File name: NH-Ade_Faisal-etal-2011.docx (1.15M)

Word count: 13746

Character count: 71390

26

Influence of large dam on seismic hazard in low seismic region of Ulu Padas Area, Northern Borneo

26

Ade Faisal · Taksiah A. Majid · Fauziah Ahmad · Felix Tongkul · Syafrina Mayang Sari

35

Received: 4 January 2010 / Accepted: 2 February 2011 / Published online: 25 February 2011
© Springer Science+Business Media B.V. 2011

Abstract The seismic hazard assessment of a site that lies in the low seismic region affected by the future existence of a large dam has been given less attention in many studies. Moreover, this condition is not addressed directly in the current seismic codes. This paper explains the importance of such information in mitigating the seismic hazard properly. Ulu Padas Area in Northern Borneo is used as an example for a case study of a site classified as a low seismic region. It is located close to the border of Malaysia, Brunei Darussalam, and Indonesia and may have a large dam in the future as the region lies in hilly geography with river flow. This study conducts probabilistic and deterministic seismic hazard analyses, and reservoir-triggered seismicity of a site affected by the future existence of a large dam. The result shows that the spectrum acceleration of the maximum design earthquake for the investigated site in the Ulu Padas Area in Northern Borneo is taken from the reservoir-triggered seismicity earthquake at short periods and from the current condition at longer periods.

Keywords Northern Borneo · Seismic hazard · Low seismic region · Large dam effect

1 Introduction

In most cases, the seismic effect on infrastructures (i.e., buildings) built on a site in a low seismic region is neglected as there is no or few evidence showing its harmful effect on the

Ade Faisal · T. A. Majid (&) · F. Ahmad
Disaster Research Nexus, School of Civil Engineering, Universiti Sains Malaysia (USM),
14300 Nibong Tebal, P. Pinang, Malaysia
e-mail: taksiah@eng.usm.my

40

ongkul
School of Science and Technology, Universiti Malaysia Sabah (UMS), No. 2073 Locked Bag,
88999 Kota Kinabalu, Sabah, Malaysia

Ade Faisal S. M. Sari
Fakultas Teknik, Universitas Muhammadiyah Sumatera Utara (UMSU), Jl. Mukhtar Basri No. 3,
Medan 20318, Indonesia

people in its recorded earthquake history. In the past decade, the increasing demand for an environment secured from natural hazards has led many researchers to investigate the level of seismic hazard in low seismic regions around the world, such as Germany, Belgium, Spain, Singapore, West Malaysia, Thailand, and the Korean Peninsula (Leydecker and Kopera 1999; Atakan et al. 2000; Balendra et al. 2002; Petersen et al. 2004; Han and Choi 2007; Lantada et al. 2010; Ornthammarath et al. 2010). Their studies were based on the historical evidence of extensive damage and loss caused by a predominantly stable plate (i.e., intra-plate) and of low seismic regions experiencing infrequent earthquakes (Anbazhagan et al. 2009). Given the absence or insufficient documentation of the occurrence of killer earthquakes in low seismic regions, there is no proper code regulating the involved parties in the development of structures in some countries in this region. This absence may give rise to problems in the future if it is not handled carefully, particularly when the creation of large dams is an option for water reserve and electrical power in developing countries (e.g., Malaysia and Brunei Darussalam). However, the common plan of development of large dams in a low seismic region is not in line with or is not even embedded in the development of their own seismic code.

Northern Borneo, a region where the borders of three countries namely Malaysia, Brunei Darussalam, and Indonesia lie, is affected by both regional and local earthquakes. Significant earthquakes from the Sulu and Celebes seas are periodically felt as slight tremors in Sabah. The NEIC (2007) earthquake database shows a total of 221, with $M \leq 6$ within 1,000 km from Kota Kinabalu since 1973 (Fig. 1). The source of regional earthquakes for Sabah comes from the active subduction zones marked by the Manila Trench, Negros Trench, Sulu Trench, Cotabato Trench, and North Sulawesi Trench.

From 1897 until today, about 28 local light to moderate earthquakes are recorded onshore Sabah and about 33 earthquakes are recorded offshore of Sabah (South China Sea, Sulu Sea, and Celebes Sea). The earthquakes have magnitudes ranging from M_b 4.0 to 5.8. The epicenters of the earthquakes are concentrated on the East Coast of Sabah, around the Lahad Datu and Ranau area. The earthquakes are mainly shallow in depth (≤ 70 km), whereas those offshore tend to be intermediate (70–200 km) in depth. The local earthquakes in Northern Borneo are related to active faults (JMGM 2006). Limited earthquake focal mechanism solutions provided by the USGS show oblique reverse faults, normal faults, and strike-slip faults responsible for the local earthquake in Sabah (Fig. 2). Two main seismic zones trending northeast–southwest occur in Sabah, specifically Ranau-Labuk Bay Zone and Semporna-Dent Peninsular Zone. Both seismic zones are characterized by northeast–southwest trending reverse faults, possibly a southeastward extension of the Cagayan Thrust and Sulu subduction in the Sulu Sea region.

Three light earthquakes were recorded within 100 km radius of the Ulu Padas Area where the large dam is assumed to be located. One occurred near Pensiangan with a magnitude M_b 4.1, Kuala Penyu (M_b 4.5), and Long Semado, Sarawak (M_b 4.5). The Pensiangan and Long Semado earthquakes appeared to be associated with a southward extension of the northeast–southwest trending Ranau-Labuk Bay seismic zone.

The objective of this study is to determine whether there is an escalation of seismic hazard for the purpose of design and assessment of regular building in a low seismic region that may have a large dam in the future. As reflected in ICOLD (2004), the increase in seismic hazard analytically is possibly due to the existence of a large dam, but it cannot increase the seismic hazard geologically. This study demonstrates the possibility of a seismic hazard increment using the Ulu Padas Area in Northern Borneo as study case of a low seismic region, which has a lack of seismic data. It runs probabilistic (PSHA) and deterministic (DSHA) seismic hazard analyses along with the reservoir-triggered

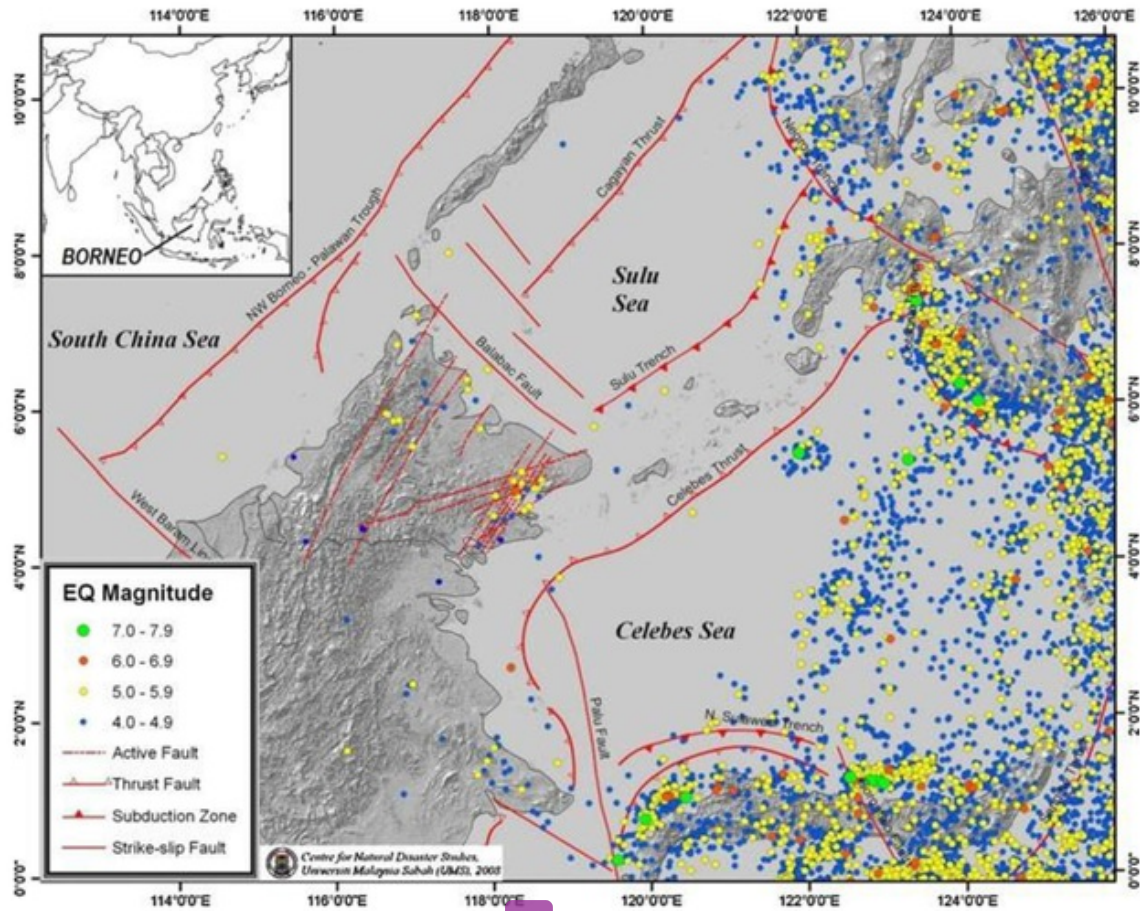


Fig. 1 Seismicity surrounding Northern Borneo based on USGS/NEIC and JMG Databases. Earthquakes onshore Northern Borneo are associated with NE-SW trending faults

seismicity (RTS) to define the maximum design earthquake (MDE) to the area when there is a possibility of building a large dam in the future.

2 Geological settings and structural geology

2.1 Seismotectonic setting

Three major tectonic plates rim Northern Borneo, namely the Eurasian Plate to the North, the Indian-Australian plate to the West and South, and the Pacific-Philippine Sea Plate to the East (Fig. 3). The GPS measurement of Michell et al. (2000) shows that the three plates converge at different directions and rates. The Sundaland and South China Sea Basin (stretched continental margin) of the Eurasian Plate slides to southeastward at a rate of about 5 cm/year, whereas the Indian-Australian and the Philippine Sea-Pacific Plates move northerly at a rate of about 7 cm/year and 10 cm/year, respectively. Active subduction zones and strike-slip faults are associated with the interactions of these three tectonic plates.

Northern Borneo sits on the semi-stable South China Sea Basin and is, to a certain extent, influenced by the active mobile belts in Sulawesi and the Philippines (Fig. 4). The active Sulu Trench subduction zone continues to East Sabah. Similarly, the active Palu Fault in Sulawesi appears to continue to East Sabah. Walpersdorf et al. (1998) show that

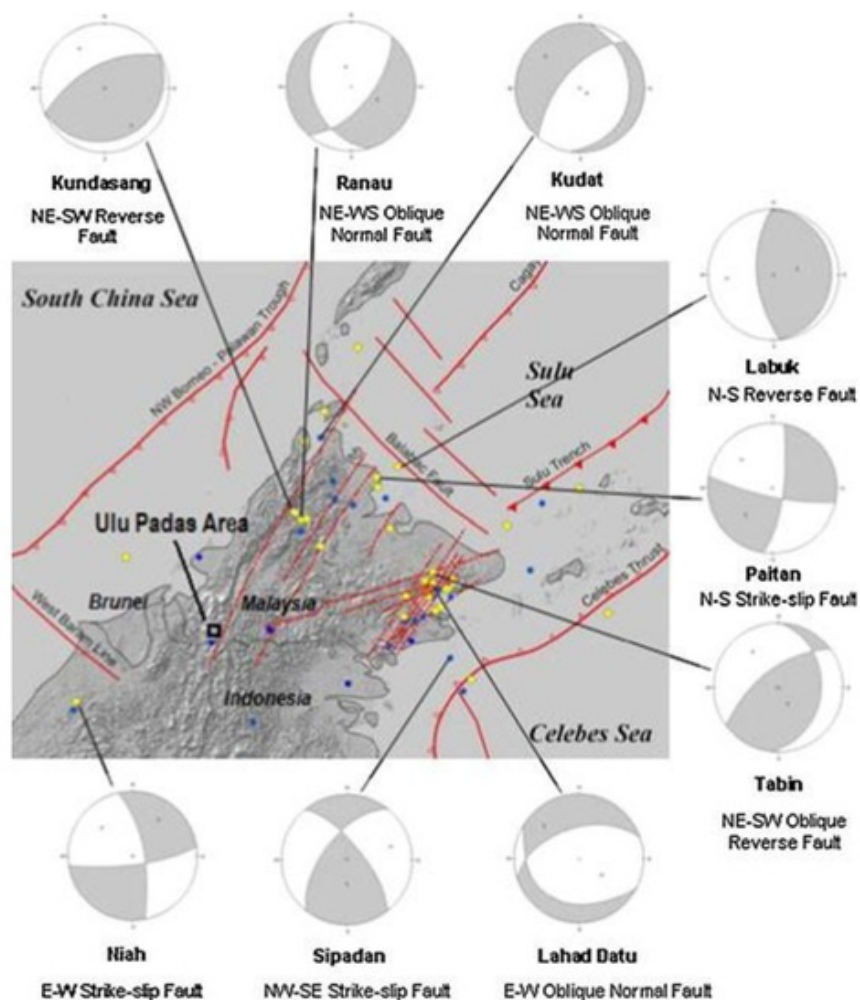


Fig. 2 Focal mechanism solutions of shallow earthquake around Northern Borneo associated with reverse, normal, and strike-slip faults. Focal mechanism based on JMGM (2006)

the GPS measurement of movement across the Palu-Koro fault exhibits a 3.4 cm/year sinistral strike-slip movement. In the South China Sea, the northwest Borneo Trough, which was probably once associated with subduction zone, is not seismically active. Active thrust faults found along the trough may mostly be associated with sedimentary loading and slumping or crustal shortening.

Large dam and Ulu Padas Area sites are assumed to be situated above a low-seismically active region with no active fault found crossing the site. Earthquake events demonstrate that the closest hypocentral event to Ulu Padas Area is 55 km for earthquake Mb 4.5. Some lineaments are found near the Ulu Padas Area. Unfortunately, no field investigation report has been found to confirm whether the lineaments are related with Quaternary fault activity. Meng (1999), however, shows that Quaternary alluvium exists at the Tenom region near the site and dam based on Tongkul's (1993, 1997) studies. We assumed that the lineaments trending from North to South might be related with Quaternary or recent tectonic activities, which are supported by Mb 4.5 earthquake 55 km away from the site. No information on the length of the rupture surface (or slip length) of the active fault's segment is found in this case.

Seismicity within a radius 500 km from the Ulu Padas Area is dominated by shallow earthquakes (depth \leq 70 km), which mostly occur in the East Coast of Sabah and in the

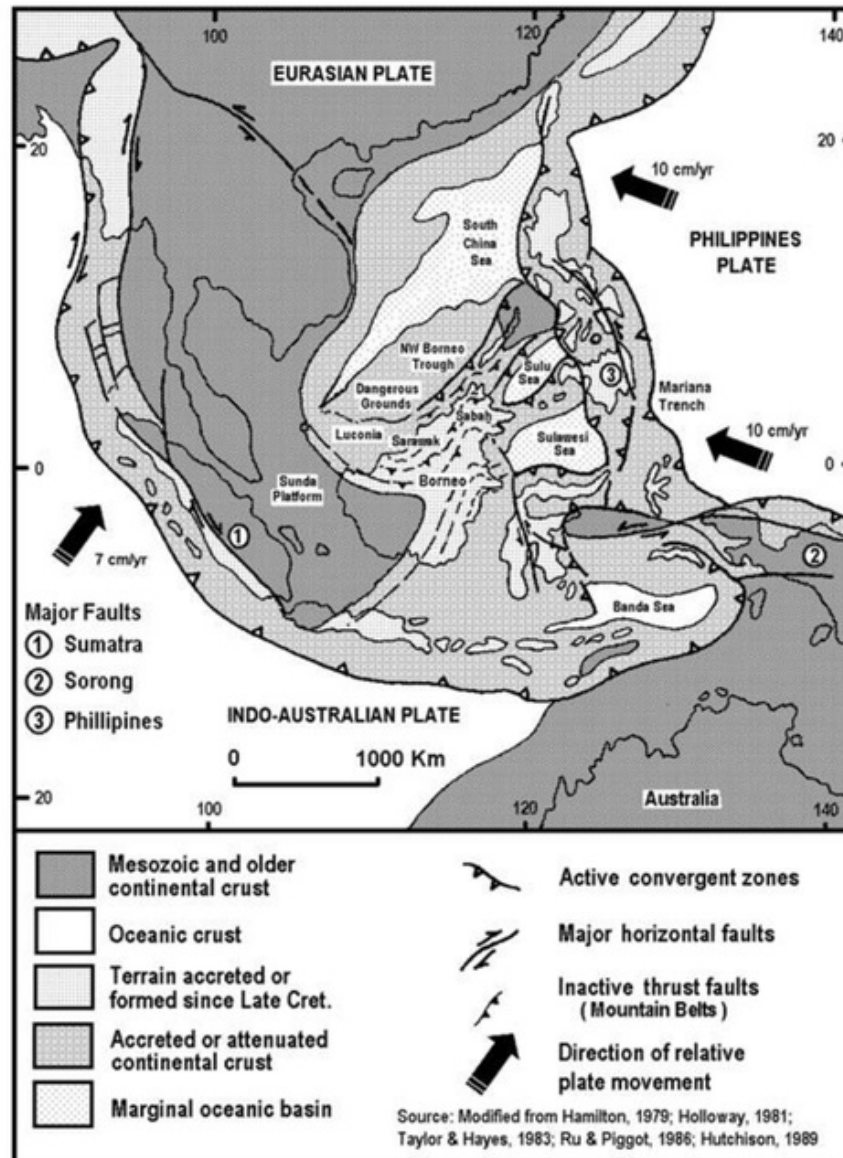


Fig. 3 Major tectonic plates surrounding Northern Borneo (Tongkul 1999)

Makassar straits region (Sulawesi). In the Sulawesi region, the earthquakes are mostly produced by the Palu-Koro Fault, which is a strike-slip fault, whereas in the East Coast of the Sabah region, they occur in Lahat Datuk Fault (or Tabin Fault), Mensaban Fault (Kundasang-Ranau Fault), and Crocker Fault Zone. This region has produced 83 earthquake events from 1963 to 2008, with magnitudes ranging from Mb 4.0 to 5.8 and mostly dominating in Sabah’s West Coast. Three light earthquakes were recorded within 100 km radius of the Ulu Padas Area where the dam is located. One occurred near the Pensiangan with a magnitude Mb 4.1, Kuala Penyu Mb 4.5, and Long Semado, Sarawak, Mb 4.5. The Pensiangan and Long Semado earthquakes appeared to be associated with a southward extension of the northeast–southwest trending Ranau-Labuk Bay seismic zone.

2.2 Structural geology

The regional structural trend of Northern Borneo is complex. However, two dominant trends can be identified onshore (Fig. 5). In western Sabah, northeast–southwest

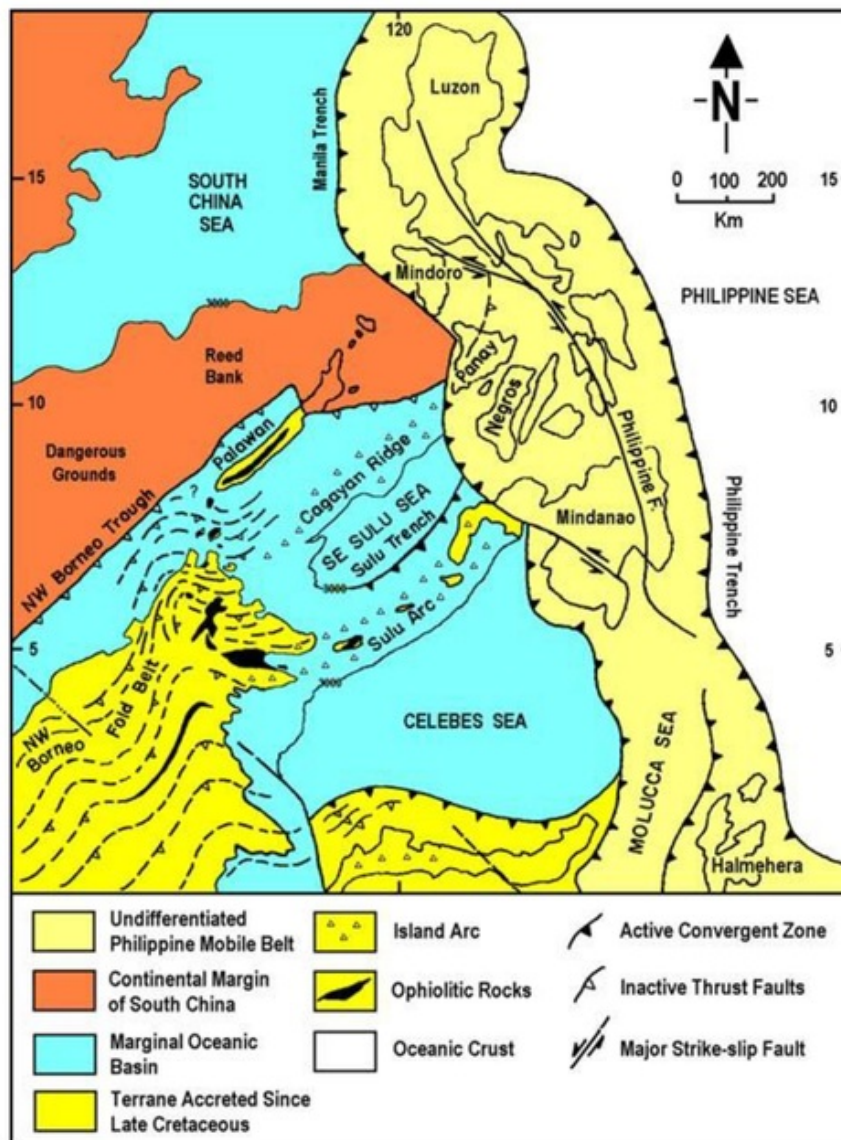


Fig. 4 Major tectonic elements surrounding Northern Borneo (Tongkul 2006)

lineaments predominate, while in northern and eastern Sabah, northwest–southeast trending lineaments that curve northeast toward eastern Sabah predominate. These lineaments mainly represent the pre-Neogene fold and thrust belt of the Crocker Formation. The fold and thrust belt extends further west offshore along the northwestern continental margin of Sabah and northeast to Palawan and northwest Sulu basin. The continuation of these fold belts offshore in eastern Sabah is uncertain. Associated with these lineaments are northwest–southeast, north–south, and northeast–southwest wrench or strike-slip faults. These dominant structures are the result of several major episodes of deformation affecting the basement rocks, pre-Neogene, and Neogene sediments. It is often difficult to differentiate between older structures and younger structures once they are reactivated. The occurrence of mud volcanoes and earthquakes along some of these northeast–southwest trending faults indicates recent movements.

The Padas Valley area forms part of the Northwest Borneo geosyncline extending from West Sarawak (Malaysia and Brunei Darussalam) and the adjacent part of Kalimantan (Indonesia) to the western and northern parts of Sabah (Malaysia). Sedimentation in the

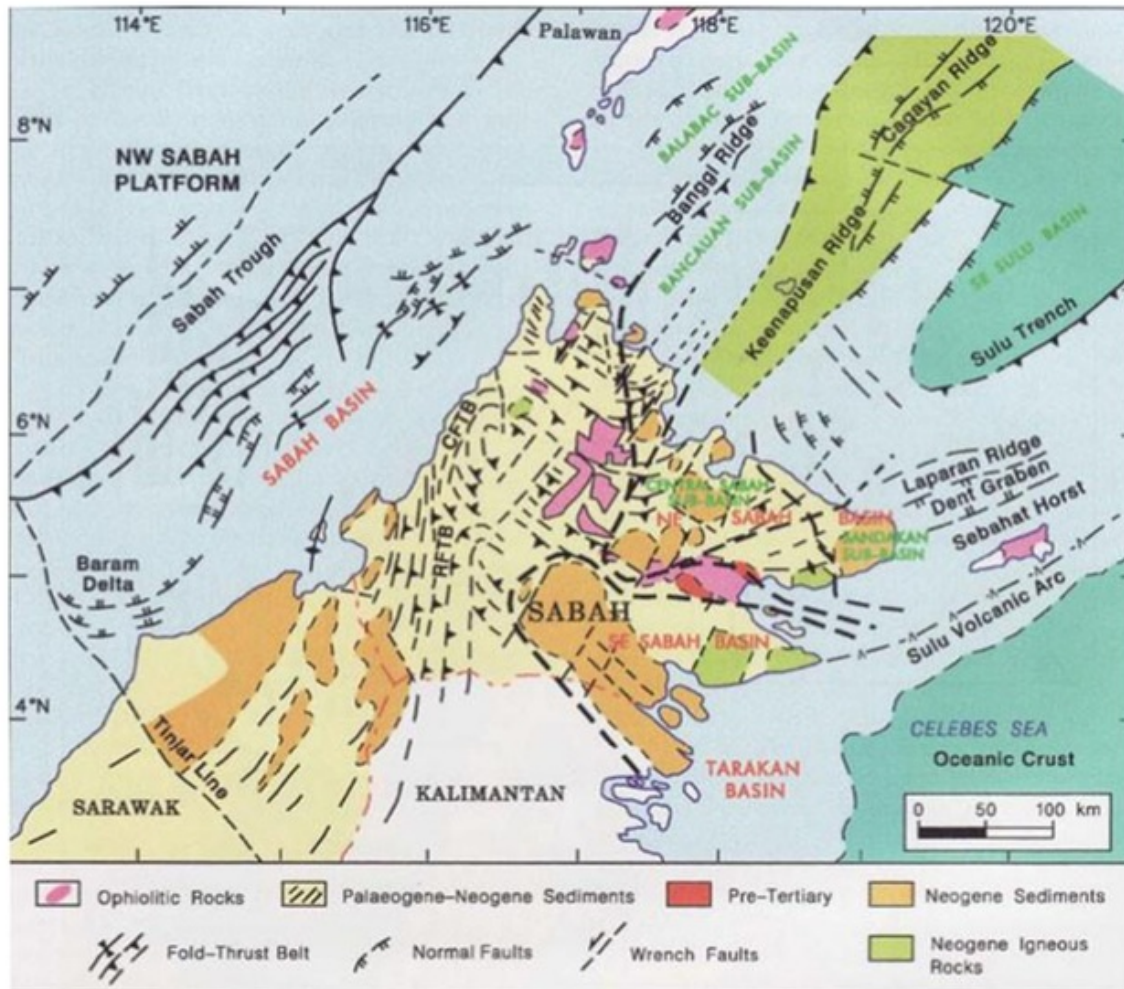


Fig. 5 Structural elements surrounding Northern Borneo (Tongkul 1993). Several NE–SW trending strike-slip faults cut through the Paleogene and Neogene sediments

geosyncline continued in the Padas Valley area throughout the Oligocene and toward the end of Miocene period. The material deposited is considered to include two distinct facies, the Crocker Formation, which is dominantly arenaceous, and the Temburong Formation, which is mainly argillaceous. The major part of these sedimentary deposits is composed of flysch-type sandstone and shale.

3 Method of analysis

The site-specific seismic hazard assessment for Ulu Padas Area in Northern Borneo (inside the State of Sabah, Malaysia) that will be having a large dam consists of the following general steps: (1) assessing the available data of the geology of earthquake fault and dam site; (2) selecting the suitable attenuation relationship; (3) collecting the earthquake event data (catalog study); (4) PSHA; (5) DSHA; and (6) RTS analysis. Ulu Padas Area is located at coordinate longitude of 115.8° East and latitude 4.8° North. The large dam is assumed to be built somewhere near the active fault at downstream of Ulu Padas Area and will have a water level height of 120 m in its reservoir, water volume of $700\text{--}1,000 \times 10^6 \text{ m}^3$, and reservoir length of about 8–10 km. No active fault was assumed beneath the large dam and

Ulu Padas Area. The closest hypocentral distance of the active fault to the investigated site is 3 km.

3.1 Selection of predicted attenuation relationship

For evaluation, attenuation relationships are selected from available predictive relationships published from 1980 to 2008 based on the seismology criteria proposed by Cotton et al. (2006). The complete report of some published predictive relationships (for 1980–2002) is well explained in Douglas (2003). The selection is also limited to those formulas that are available in the PSHA program. The range of applicability of the eleven selected attenuation models is explained in the results section.

The weighting of the selected model follows the Scherbaum et al.'s (2005) method to obtain proper ranking. However, this study only employed a partial procedure that was applied in Scherbaum et al. as Ulu Padas Area as a target model has very little information related to its seismologic properties. In this study, the weights are assigned to some indicators in the candidate attenuation equations, which reflect the relative confidence of the analyst in each of the models providing the best estimate for ground motions considered in the hazard analysis. The criteria used reflect the reliability of the equation to predict ground motions at a particular response frequency and for a given range of magnitudes and distances in the host region.

Based on the available tectonic and seismologic knowledge of the Ulu Padas Area site, we used some parameters as criteria in selecting the suitable attenuation model, namely magnitude M_b 4.0–6.2, hypocentral distance $R \leq 500$ km, shallow crustal earthquake (normal, reverse, and strike-slip faults), rock site, intraslab earthquake, and stable continental region. We used a dam fundamental frequency within the range of 4–15 Hz as an additional indicator. We also assumed that intraslab earthquakes within the considered radius from the site are much like the Central Europe or East/Central US earthquakes. The shear wave velocity of the bedrock of site was assumed to be 760 m/s, which lies within the range of soft rock to hard rock types of NEHRP 2000 (BSSC 2001).

The information on the knowledge base and the target condition is used to assign a descriptive measure of quality for each equation and category. Such measures may be *Good*, *Fair*, or *Poor* (quantitatively equal to 3, 2, or 1, respectively). The weights of this model are called Expert's Weight and are considered as Scenario 1 in the selection of the attenuation model. For Scenario 2, we assume no treat is done to differentiate the relative degrees of applicability of the equations and assigns equal weights; this is called Equal Weight. Scenario 3 employs weights without any scientific criteria, which are randomly generated weights assigned with the term Random Weight. To emphasize the use of non-overlapping data sets but still cover roughly the same geographic regions as the full set of attenuation models, an additional scenario is defined by only using attenuation models representing four regions: Worldwide, Europe, Eastern North/Central-Eastern North America (ENA/CENA), and Western North America (WNA). This is Scenario 4, which we call Independence Weight. The final weight is obtained by summing up the scenario's weights and normalizing them with the total weight. We rank the eleven attenuation models suitable for the Ulu Padas Area based on this Final Weight and use them in the logic tree analysis.

In DSHA, the use of single attenuation model is commonly practiced. However, the application or conversion of single model of a region to the different region would introduce epistemic uncertainty since the relationship of model is theoretically valid in terms of its derivation and empirical basis (Scherbaum et al. 2005). The epistemic

uncertainty due to conversion of model from high to low seismic (other) region could artificially increase the hazard as well (Wiemer et al. 2009). Therefore, this study employed a composite model using eleven attenuation relationships that selected and weighted based on the procedure as proposed by Scherbaum et al. (2005) in order to reduce the uncertainty and to be more comparable with the uniform hazard spectra of PSHA. The criterion was based only on site condition as well as magnitude and distance range. The maximum credible earthquake (MCE) ranged from Mb 4.1 to 5.4, while the hypocentral distance ranged from 55 to 160 km. The investigated site was assumed at bedrock with 760 m/s of shear wave velocity.

3.2 Deterministic method

A site-specific DSHA is generally conducted through the following steps (Reiter 1990; Krinitzky 1995, 2002):

- Conduct the identification and characterization of all earthquake sources with their source-to-site distance that may affect the site and that are capable of producing significant ground motion.
- Choose the appropriate ground motion model (attenuation function) to predict the ground motion parameters at the site as a function of magnitude, distance, and site condition.
- Select the earthquake that produces the strongest level of motion (also called the controlling earthquake) by comparing the motion produced by the earthquake magnitude and its source-to-site distance identified in the previous step.
- Characterize the hazard at the site using the peak ordinates of the response spectrum acceleration. Select the largest earthquake event that can be reasonably expected to occur for each source and assign it as the maximum credible earthquake (MCE), which is usually taken at the median or the median-plus-one-standard-deviation (84th-percentile) value. For critical structures, such as a dam, the mean-plus-one-standard-deviation value can be selected if the site is near a very active fault (FEMA 2005).
- Select analogous accelerogram records considering the magnitude, distance, fault mechanism, and site condition to represent the earthquake excitation at the site.

According to ICOLD (1989), an MCE is generally defined as an upper bound of the expected magnitude or as an upper bound of the expected earthquake intensity. A DSHA or probabilistic method can be used to evaluate the MCE (FEMA 2005; ICOLD 1989). The MCE is used as the largest possible earthquake along a recognized fault under the presently known or presumed tectonic framework (FEMA 2005). However, the earthquake coming from the result of the PSHA may become the MCE. In practice of large dam seismic analysis, this MCE is considered to have a return period earthquake (RPE) of several thousand years, typically 10,000 years in a region of low to moderate seismicity, and is defined probabilistically (Wieland 2004, 2005). ICOLD (2004) suggests to use the term safety evaluation earthquake (SEE) rather than to use MCE in seismic risk analysis of large dam. However, we kept using term MCE since the intention is for the site and it is commonly used in practice.

In this study, we regard all faults as potential sources for future earthquakes if they have proven or probable evidence for movement in about 35,000 to 100,000 years (FEMA 2005) or Quaternary time (ICOLD 1989). However, the very limited existing fault activity information in Ulu Padas Area, Northern Borneo, results in major uncertainties on the average fault slip rate, rupture length of the fault, magnitude of earthquakes associated

with past fault movements, average surface faulting earthquake recurrence interval, and time of the last coseismic surface fault rupture. These uncertainties make the prediction of maximum earthquake in DSHA using the seismologic parameters (rupture length, width, or area) impossible to apply. The intensity report within the area of the site and large dam site is not available as well. Hence, MCE on the bedrock for the investigated site is determined using the available historical earthquakes from recent event catalogs (1963–2008).

3.3 Probabilistic method

In general, the PSHA is comprised of the following five steps (Reiter 1990; McGuire 2004):

- Identify all earthquake sources capable of producing damaging ground motions.
- Characterize the distribution of earthquake magnitudes (the rates at which earthquakes of various magnitudes are expected to occur).
- Characterize the distribution of source-to-site distances associated with potential earthquakes.
- Predict the resulting distribution of ground motion intensity as a function of earthquake magnitude, distance, and so on.
- Combine uncertainties in earthquake size, location, and ground motion intensity using the calculation known as the total probability theorem.
- Define the controlling earthquakes by disaggregating the total hazard for all point considered in spectrum acceleration.

Earthquake sources can be faults, which are typically planar surfaces identified through various means such as observations of past earthquake locations and geological evidence. As individual faults in the Northern Borneo region are not identified clearly, earthquake sources are described by area regions in which earthquakes may occur anywhere within a radius 500 km [ICOLD (1983) indicates at least 300 km] from the Ulu Das Area.

Once all possible sources are identified, we identified the distribution of magnitudes and source-to-site distances associated with earthquakes from each source. The distribution of earthquake sizes in a region is assumed to follow the Gutenberg–Richter recurrence law (Gutenberg and Richter 1944). The Gutenberg–Richter's constants are estimated using the statistical analysis of historical earthquake event observations provided by USGS. As the observed events are truncated in maximum and minimum earthquake magnitude, $M_{\min} \leq M \leq M_{\max}$, the exponential recurrence model is used in determining the number of earthquake magnitude M per unit time following McGuire (2004). The maximum likelihood of the activity rate is assumed under Poisson's distribution. Further explanation of the method can be found in McGuire (2004). The EZ-FRISK™ (RiskEngineering Inc 2008) program is used in the probabilistic seismic hazard analysis.

ICOLD (1989) and FEMA (2005) state that the MCE of a dam, in this study we apply to the site, may come from an earthquake based on the result of the PSHA result. As this study deals with low seismic hazard, we selected the controlling earthquake on the bedrock from PSHA 475 years RPE as MCE. For comparison purpose, the controlling earthquake from 2,475 years RPE is presented as well. In moderate earthquakes, especially earthquakes with a magnitude of more than 6, the DSHA result in determining the peak ground acceleration (PGA) is mostly higher than the result of PSHA.

3.3.1 Epistemic uncertainty

In seismic hazard analyses, epistemic uncertainty is used to limit data (often very limited) and is considered by using alternative models and/or parameter values for the source characterization and ground motion attenuation relation. For each combination of alternative models, the hazard is recomputed resulting in a suite of alternative hazard curves. As an area of low-to-moderate seismicity, for example Northern Borneo, is often the case wherein many equations are needed to capture the epistemic uncertainty, this gives greater significance to the issue of selecting these equations rather than to assign their relative weightings subsequently (Sabetta et al. 2005).

This study develops the logic tree to be incorporated with PSHA to capture epistemic uncertainty, as shown in Fig. 6. There are four main epistemic uncertainties: recurrence model, seismic source, magnitude conversion, and maximum magnitude. No characteristic recurrence model is used in this analysis. The weighting process of this logic tree is influenced greatly by Scherbaum et al.'s (2005) study. The weighting value of the attenuation model comes from the previous attenuation selection process. There are 78 scenarios of epistemic uncertainty for the current condition and 131 scenarios for the condition with the large dam effect employed in this study. The weight from attenuation model selection is used in weighting the attenuation model uncertainty. The maximum magnitude is added 0.5 to capture the uncertainty of this parameter (McGuire 2004). The magnitude scale conversion cannot be avoided and hence Utsu (2002) relationship is used. Since the conversion contributes another uncertainty in the analysis, a weight of 0.6 is given when the magnitude is not converted. It means that the M_b values in the earthquake catalog are assumed to be the same with M_w , which is the formal magnitude scale used in most considered attenuation models.

3.4 Reservoir-triggered seismicity

The artificially induced phenomena related to the impoundment of bodies of water known as RTS is mostly linked with normal and strike-slip fault. If the causative fault is already critically stressed, it is logical to consider that the increase in shear stresses and the reduction in effective normal stresses due to the weight of water reservoir and additional pore pressures, respectively, can trigger seismic activity. In cases of normal and strike-slip faults, this influence has a tendency to place the representative Mohr circle nearer to the failure slope, such as a decrease in shear strength along the fault (ICOLD 2004). From a worldwide standpoint, only a small number of reservoirs impounded by large dams have triggered known seismic activity.

Currently, the RTS phenomena are not a clear knowledge that can be used in predicting seismic hazard for seismic design and/or seismic assessment of a dam. It has significantly high aleatory and epistemic uncertainties. It is a clear and widely accepted fact that a rigorous analysis to predict a reliable magnitude and location of RTS is hardly feasible, considering the nature of the parameters involved (USCOLD 1997; FEMA 2005; ICOLD 2004). In this study, the seismic potential at Ulu Padas Area was assumed to be governed by its tectonic conditions and would not be increased by RTS (ICOLD 2004). A prediction of the occurrence and magnitude of RTS is based on recent information related to the reverse fault activity near the dam site, reservoir water level height of 120 m, volume of reservoir of $700\text{--}1,000 \times 10^6 \text{ m}^3$, and reservoir length of 8–10 km.

Using the above-mentioned facts, we predict the RTS using recent information mainly from the cases of RTS in the following references:

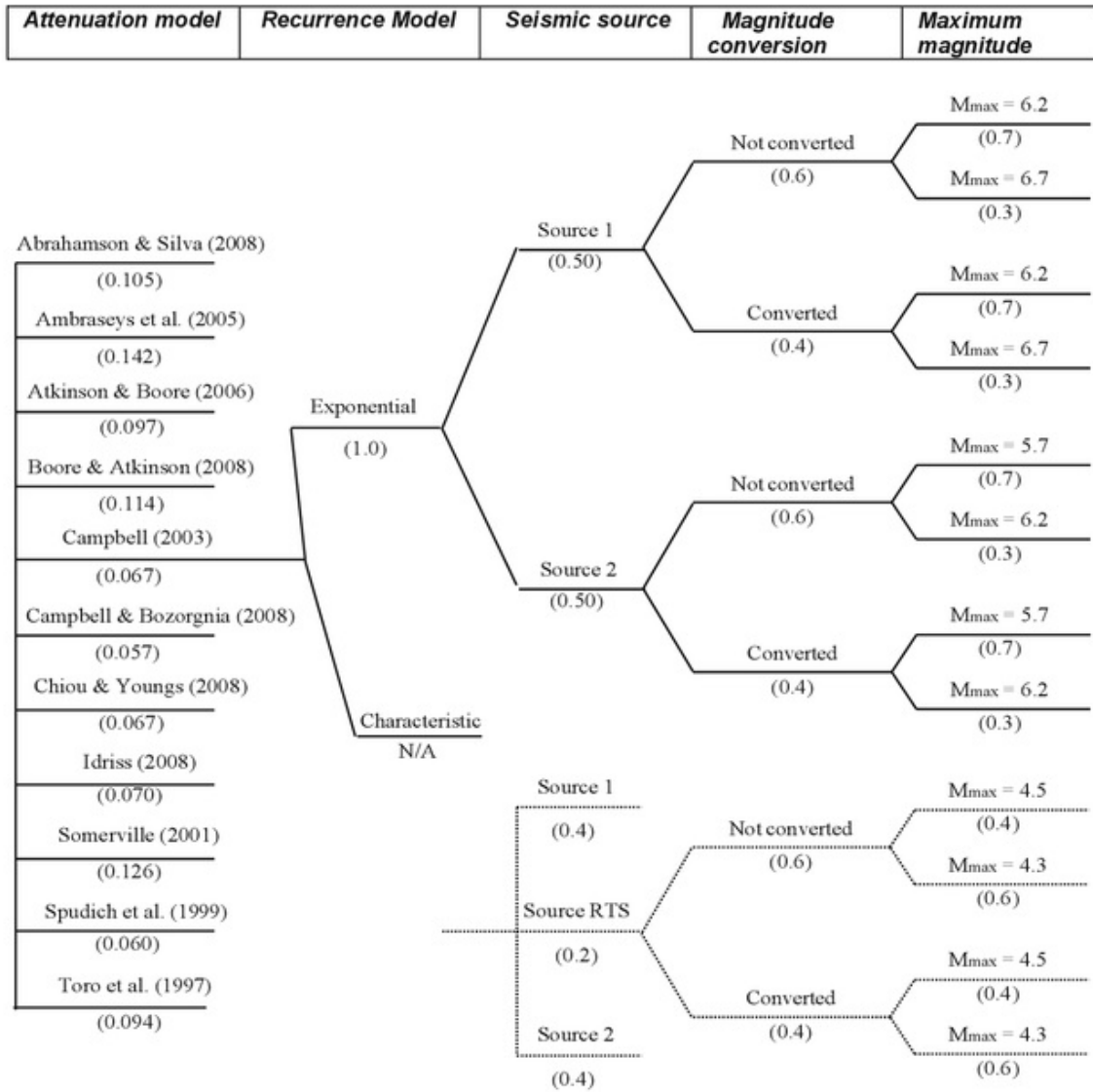


Fig. 6 Logic tree for epistemic uncertainty in PSHA. Dashed line indicates the scenario used for the condition with large dam effect

- ICOLD (2004) modified from USCOLD (1997). It is originally from Baecher and Keeney (1982) based on the water level and volume of a reservoir having RTS
- Simpson et al. (1988) based on the water level and earthquake occurrence
- McGarr et al. (2002) based on the length of reservoir and magnitude.

The RTS earthquake is supplied to the probabilistic seismic hazard analysis (PSHA), with the seismic source area located in a region near an active fault. The Ulu Padas Area is situated outside this seismic source with a 3-km epicentral distance. Accommodating this seismic source into the PSHA can be difficult because it has no historical record, whereas the criteria of a seismically active fault are defined based on the geological assumption only, as indicated in Sect. 2. Estimating the magnitude using a ground motion model through the stochastic method is also not possible due to the insufficient data. Therefore, we assumed that low earthquakes have occurred that would be used in calculating the annual rate of occurrence. The annual rate is constrained to be less than those of the other source areas to show that the event is very rare in the considered area. The minimum magnitude is set to Mb 4.0 for this seismic source, whereas the maximum magnitude is

taken from the predicted RTS earthquake. The b -value, a Gutenberg–Richter constant that describes the relative likelihood of large and small earthquakes, of the RTS source is normally higher than its regional seismicity (Gupta 2002). Hence, the additional events with magnitude slightly higher than minimum magnitude are estimated and adjusted so that the b -value of the RTS source is higher than those of source areas 1 and 2.

Given that this procedure introduces significant uncertainties, we assigned a lower weighted value to the RTS seismic source than to the other seismic sources areas. We also assumed that two magnitudes govern the RTS seismic source, M_b 4.5 and M_b 4.3 with weighted values of 0.4 and 0.6, respectively, to reduce the excessive superiority of the short-distance events introduced by the maximum magnitude to the total seismic hazard. This also led us to lower the weighted RTS seismic source compared with the other sources (Fig. 6).

3.5 Maximum design earthquake

For seismic safety considerations, the site in the Ulu Padas Area should be designed or analyzed using the maximum level of ground motion produced by the MDE according to ICOLD (1989, 2004) and FEMA (2005) because a large dam will be built near the active fault, and the lineament of this active fault is trending close to the site. Usually, MDE is calculated by controlling the MCE for high-hazard potential dams. However, for low- or significant-hazard dams, the MDE may be determined based on faults active in the Holocene period or according to other agency-specified criteria (FEMA 2005). The MDE may be set equal to the MCE, equal to 10,000-year earthquake (PSHA), equal to predicted earthquake due to RTS, or equal to a design earthquake less than the MCE depending on the circumstances (ICOLD 1989, 2004; FEMA 2005). In selecting the MDE, indicating that only earthquakes with 2 and 10% probability of exceedance in the 50 years lifetime design, that is, 475 and 2,475 years RPEs, respectively, are considered as the controlling earthquakes or MCE from the PSHA. Although the use of a mean scenario as the controlling earthquake has its advantage, a mode scenario was selected in this study to represent the controlling earthquake of 475 and 2,475 years RPEs. The mode scenario demonstrates the event that most likely generates the exceedance of the target ground motion level at the considered site (Bazzurro and Cornell 1999; Abrahamson 2006).

In the DSHA of a high seismic region such as California, the MDE should be developed from the MCE at the median for a regular building design and 1.5 times the median or median-plus-one-standard-deviation value (84th-percentile) for important or critical structures when the largest earthquake that can be reasonably expected is considered (Krnitzsky 2002; FEMA 2005; Zheming Wang, written communication). However, in low seismic regions, the use of the 50th- or 84th-percentile may be too conservative because the recurrence interval for the design earthquake is too long (Zheming Wang, written communication). Moreover, the selection of the MDE is also influenced by the owner, political considerations, and economic constraints (Krnitzsky 2002).

In the seismic analysis of a dam, the MDE should be selected from the MCE based on either PSHA or DSHA, whichever produces the maximum result, as this study involves a site that may have a large dam that could produce RTS. However, in this case, we compared the DSHA result at the median value of the 475 years RPE with the PSHA (McGuire 2001) for the purpose of a seismic design or assessment of a regular building at the investigated site.

3.6 Selection of input ground motion

Earthquake ground motion represents the regional seismicity from a source mechanism to the path effect and then to the site effect. For instance, as the magnitude increases, the more the low frequency motion tends to exhibit increasingly in the frequency bandwidth and decreasingly in the corner frequency. The ground motion for seismic design and assessment is much influenced by the characteristics of the ground motion dependent on the various building design and assessment assumptions (McGuire 2004; Douglas and Aochi 2008). A great uncertainty that poses great challenges is thereby introduced. To demonstrate the effect of a large dam on the seismic hazards of a site in a low seismic region, the selection of ground motion for engineering purposes is also discussed in this study. The common method regulated in many seismic codes for engineering design (e.g., CEN 2004; ASCE 2007) is used, which consists of a selection of the ground motion records from an online available database based on seismologic parameters (Bommer and Acevedo 2004), such as the fault mechanism, magnitude, hypocentral distance, site condition (general rock), frequency bandwidth, and duration. Afterward, matching the MDE spectra using spectra-matching method (Abrahamson 1992; Hancock et al. 2006) using the SeismoMatch software (Seismosoft 2009) is performed.

In generating the synthetic ground motion through spectral-matching, frequency and duration are the strong motion parameters that should be considered. Given that the complete characteristics of the RTS strong motion are rarely reported in the literature, we assumed that a high frequency is dominant in the RTS ground motion because it is similar to a natural earthquake motion produced by low-magnitude near-field earthquakes. The RTS earthquake is also associated with local seismicity and a very shallow event (Chadha et al. 1997; Talwani 1997). A natural ground motion with a longer distance in a seismic region without RTS is not easy to assume because it is associated with a distant earthquake containing a complex frequency type due to the travel path and site effects. We also considered the RTS motion to have a short duration (uniform duration type) of less than 10 s, whereas a natural ground motion for distant earthquakes has a long duration. A short-duration event is related to a low magnitude and a short epicentral distance (Kramer 1996; Bommer and Martinez-Pereira 1999). The event was also selected based on the RTS aftershock earthquake M 4.5 at the Hsinfengkiang Dam in China (Bolt and Cloud 1974) and earthquakes with various durations as reported by Jobry et al. (1978) and Kramer (1996). The strong motion record was selected from the Internet Site for European Strong-Motion Data (ISESD) (Ambraseys et al. 2001) and the PEER Strong Motion Database (PEER 2000).

4 Analyses and discussion

4.1 Selected attenuation model

We selected eleven attenuation models, namely Abrahamson and Silva (2008), Ambraseys et al. (2005), Atkinson and Boore (2006), Boore and Atkinson (2008), Campbell (2003), Campbell and Bozorgnia (2008), Chiou and Youngs (2008), Idriss (2008), Somerville et al. (2001), Spudich et al. (1999), and Toro et al. (1997). These models are dominated by the model on the rock site condition and with a magnitude type of moment magnitude (M_w). The assumed validity range of the above criteria is fully explained in Table 1. In Tables 2 and 3, we show our scores and the weights for each attenuation model that represents

Table 1 Attenuation models and their assumed validity ranges

No.	Model Name	<i>M</i> type	<i>M</i> range	Frequency (Hz)	<i>R</i> type	<i>R</i> range	Site Condition	Region
1	Abrahamson and Silva (2008)	Mw	5.0–8.5	0.1–100	rup	B200	Soil, Rock	Worldwide
2	Ambraseys et al. (2005)	Mw	5.0–7.0	0.4–20	jb	B100	Rock	Europe, Middle East
3	Atkinson and Boore (2006)	Mw	4.8–8.0	0.2–20	hyp	B200	Hard rock	ENA
4	Boore and Atkinson (2008)	Mw	5.0–8.0	0.1–100	jb	B200	Soil, Rock	Worldwide
5	Campbell (2003)	Mw	5.0	0.01–4.0	hyp	B1000	Hard rock	ENA
6	Campbell and Bozorgnia (2008)	Mw	4.0–8.5	0.1–100	hyp	B200	Soil, Rock	WNA
7	Chiou and Youngs (2008)	Mw	4.0–8.5	0.1–100	rup	B200	Soil, Rock	WNA
8	Idriss (2008)	Mw	4.5–8.5	0.1–200	rup	B200	Rock	Worldwide
9	Somerville et al. (2001)	Mw	6.0–7.5	0.25–100	jb	B500	Hard rock	ENA, CNA
10	Spudich et al. (1999)	Mw	5.0–7.0	0.5–10	jb	B100	Rock	Worldwide
11	Toro et al. (1997)	Mw	5.0–8.0	1–35	jb	B500	Mid-continent	ENA, CNA

Expert Weight. This demonstrates that the Ambraseys et al. (2005) and Somerville et al. (2001) models agree well with the site condition, followed by Boore and Atkinson (2008), Abrahamson and Silva (2008), and Atkinson and Boore (2006).

4.2 MCE based on DSHA and RTS

Many small (3 < *M* < 5) and moderate (5 < *M* < 7) earthquakes occur in the surrounding Ulu Padas Area (Fig. 7) without clear association with a known geological fault. In DSHA, these are considered as background or random earthquakes. Generally, moderate earthquakes produce only small ground motion when located more than 50 km from the site. However, we limit our MCE determinations to the undetermined faults or earthquake sources within a radius of 160 km of the Ulu Padas Area. Based on historical events, the closer earthquake to the Ulu Padas Area site is a small earthquake (Mb 4.5) with a hypocentral distance of 45 km in seismic source 2, whereas a moderate earthquake is found 152 km away from the site with Mb 5.2. There is no complete information related to the style-of-faulting of earthquakes that occurred in seismic source 2. The complete list of selected earthquakes for DSHA is shown in Table 4.

The RTS may probably occur near the dam site with a magnitude Mb B 4.5. Although case studies in ICOLD (2004) demonstrate the fact that RTS with Mb > 5 occurs for dams with a water height of 120–130 m, the possibility of having an RTS magnitude of Mb > 4.5 at the Ulu Padas Area is very low, as the historical earthquake event near the dam site region indicates the documented absence of such activity. Moreover, this prediction of RTS is probably weak as there are very few cases of reverse type-of-faulting showing RTS (ICOLD 2004).

Table 2 Expert weighting for attenuation models based on seismologic criteria of Cotton et al. (2006)

No.	Model	M type	M range	Frequency (Hz)	R type	R range	Site condition	Region coverage	Method	Expert weights
1	Abrahamson and Silva (2008)	0.09	0.08	0.10	0.08	0.08	0.07	0.05	0.11	0.036
2	Ambraseys et al. (2005)	0.09	0.08	0.07	0.08	0.12	0.13	0.10	0.11	0.143
3	Atkinson and Boore (2006)	0.09	0.08	0.10	0.17	0.08	0.07	0.15	0.06	0.215
4	Boore and Atkinson (2008)	0.09	0.08	0.10	0.08	0.08	0.13	0.05	0.11	0.072
5	Campbell (2003)	0.09	0.08	0.03	0.08	0.12	0.07	0.15	0.06	0.054
6	Campbell and Bozorgnia (2008)	0.09	0.13	0.10	0.08	0.08	0.07	0.05	0.11	0.054
7	Chiou and Youngs (2008)	0.09	0.13	0.10	0.08	0.08	0.07	0.05	0.11	0.054
8	Idriss (2008)	0.09	0.13	0.10	0.08	0.08	0.13	0.05	0.11	0.107
9	Somerville et al. (2001)	0.09	0.04	0.10	0.08	0.12	0.07	0.15	0.06	0.081
10	Spudich et al. (1999)	0.09	0.08	0.07	0.08	0.04	0.13	0.05	0.11	0.024
11	Toro et al. (1997)	0.09	0.08	0.10	0.08	0.12	0.07	0.15	0.06	0.161
	Total	1.00	1.00	1.00	1.00	1.00	1.00	1.00	1.00	1.00

The expert weighting in Table 2 was using the following criteria

Magnitude type: Mb = Good = 3; Ms = Fair = 2; Mw = Poor = 1

Magnitude range started from: 4.0–4.5 = Good = 3; 4.6–5.4 = Fair = 2; 5.5 = Poor = 1

Frequency range up to: \ 100 Hz = Good = 3; \ 10 Hz = Fair = 2; \ 4 Hz = Poor = 1

Distance (R) type: Hypocentral (hyp) = Good = 2; else = Poor = 1

Distance R range up to: \ 150 km = Good = 3; \ 200 km = Fair = 2; \ 500 km = Poor = 1

Site condition: Rock = Good = 2; else = Poor = 1

Region coverage: ENA/CENA = Good = 3; Europe/Extensional = 2; Worldwide/WNA = 1

Methodology of model: Empirical = Good = 2; Stochastic = Poor = 1

Table 3 Rank of the attenuation model using procedure of Scherbaum et al. (2005)

No.	Model	Expert weights	Equal weights	Random weights	Independence weights	Total weights	Final weights	Rank
1	Abrahamson and Silva (2008)	0.036	0.091	0.042	0.250	0.418	0.105	4
2	Ambraseys et al. (2005)	0.143	0.091	0.083	0.250	0.568	0.142	1
3	Atkinson and Boore (2006)	0.215	0.091	0.083	0.000	0.389	0.097	5
4	Boore and Atkinson (2008)	0.072	0.091	0.042	0.250	0.454	0.114	3
5	Campbell (2003)	0.054	0.091	0.125	0.000	0.270	0.067	8
6	Campbell and Bozorgnia (2008)	0.054	0.091	0.083	0.000	0.228	0.057	11
7	Chiou and Youngs (2008)	0.054	0.091	0.125	0.000	0.270	0.067	9
8	Idriss (2008)	0.107	0.091	0.083	0.000	0.282	0.070	7
9	Somerville et al. (2001)	0.081	0.091	0.083	0.250	0.505	0.126	2
10	Spudich et al. (1999)	0.024	0.091	0.125	0.000	0.240	0.060	10
11	Toro et al. (1997)	0.161	0.091	0.125	0.000	0.377	0.094	6
	Total	1.000	1.000	1.000	1.000	4.000	1.000	

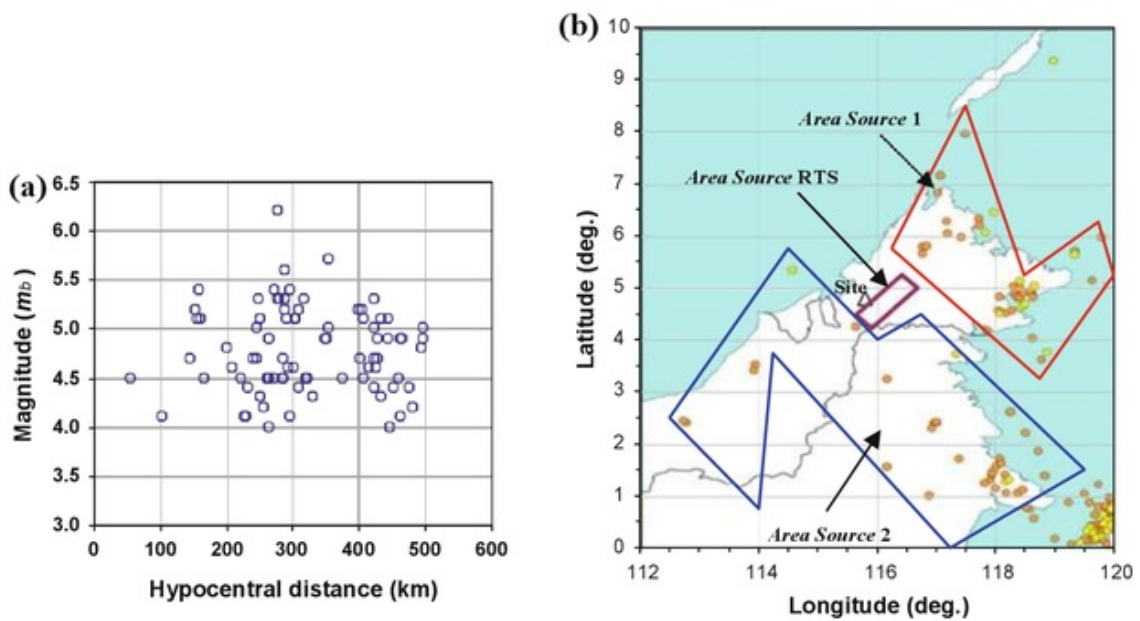


Fig. 7 Earthquake distribution and area seismic sources for the investigated site in Ulu Padas Area

The prediction of the location of RTS is similarly not well understood as the RTS itself. In general, cases of RTS present as shallow earthquakes (ICOLD 2004). These events demonstrate the tendency of a mainshock with a depth 10–20 km (Simpson et al. 1988; Gupta 2002) for a magnitude exceeding 4. However, RTS as a product of rapid response tends to have seismicity with a depth of B10 km beneath or near the edges of the reservoir but with a low magnitude. These RTS cases occurred at Nurek, Monticello, and Manic-3

Table 4 Seismic sources and the MCE earthquakes for Ulu Padas Area

Source	Magnitude	Distance	Source type	Location
1	Mb 4.7	$R = 145$ km	NE-WS-Normal	Ranau
	Mb 5.1	$R = 157$ km	NE-WS-Normal	Ranau
	Mb 5.4	$R = 159$ km	NE-SE-Reverse	Kundasang
2	Mb 4.5	$R = 55$ km	NE-SE-Reverse	Undetermined
	Mb 4.1	$R = 102$ km	Background	Undetermined
	Mb 5.2	$R = 154$ km	Background	Undetermined
RTS	Mb 4.5	$R = 10.4$ km	Background	Ulu Padas

dams (Simpson et al. 1988). Delayed response types of RTS often have seismicity with larger magnitudes and deeper depths (C10 km), with distances sometimes extending to 10 or more km from the reservoir.

For the worst case scenario, we assume that the delayed response type of RTS (Mb 4.5) will probably occur at a depth of 10 km. Since the RTS earthquake can be occurred in any point of active fault area near the reservoir, estimation of closest epicentral distance of RTS is taken based on closest distance from active fault area (RTS source) to the site in Ulu Padas Area, which is assumed to be 3 km. Hence, we predict that the controlling earthquake of RTS for the Ulu Padas Area is probably an earthquake Mb 4.5 with a hypocentral distance of 10.4 km. We added the source area containing the RTS earthquakes, henceforth RTS source, in between source areas 1 and 2, which are closer to the site and along the active fault line near the site where the RTS is assumed to occur, as shown in Fig. 7b. Using the composite ground motion models, the spectrum accelerations (SA) of the RTS earthquake at the 50th- and 84th-percentiles were estimated deterministically. The SA of the RTS earthquake at the 50th-percentile reached 0.1344 g at the PGA, 0.2860 g at a period of 0.1 s or SA(0.1 s), and 0.0163 g at a period of 1.0 s. The summary of the obtained SAs are listed in Table 5 and illustrated in Fig. 8. As expected, the RTS source

Table 5 MCE of DSHA at 84th- and 50th-percentiles (median) values for the investigated site

Source	Mag.	Distance	Style-of-faulting	PGA (g)	SA(0.1 s) (g)	SA(1.0 s) (g)	Method
1	Mb 4.7	$R = 145$ km	NE-WS-Normal	0.0065	0.0139	0.0017	84th-percentile
				0.0034	0.0069	0.0008	Median
	Mb 5.1	$R = 157$ km	NE-WS-Normal	0.0088	0.0185	0.0033	84th-percentile
				0.0047	0.0094	0.0016	Median
	Mb 5.4	$R = 159$ km	NE-SE-Reverse	0.0119	0.0248	0.0055	84th-percentile
				0.0064	0.0128	0.0027	Median
2	Mb 4.5	$R = 55$ km	NE-SE-Reverse	0.0199	0.0436	0.0035	84th-percentile
				0.0102	0.0212	0.0017	Median
	Mb 4.1	$R = 102$ km	Background	0.0057	0.0123	0.0008	84th-percentile
				0.0029	0.0060	0.0004	Median
	Mb 5.2	$R = 154$ km	Background	0.0101	0.0213	0.0040	84th-percentile
				0.0054	0.0109	0.0020	Median
RTS	Mb 4.5	$R = 10.4$ km	Background	0.2727	0.6204	0.0334	84th-percentile
				0.1344	0.2860	0.0163	Median

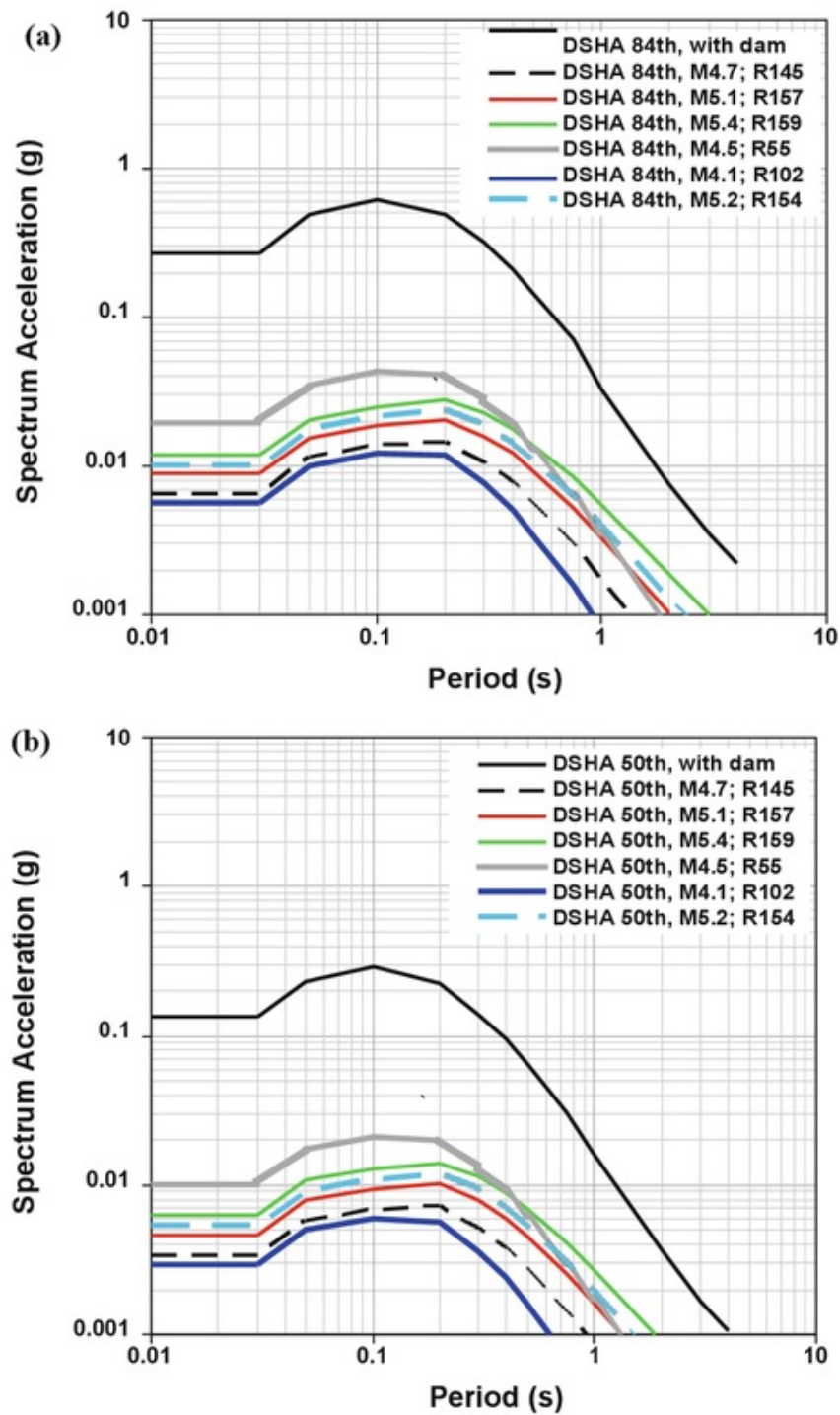


Fig. 8 Comparison spectrum acceleration based on DSHA with and without the effect of large dam: a 84th-percentile, b 50th-percentile

significantly dominated the seismic hazard of the site in Ulu Padas for the low and high periods of SA. Thus, the median value was selected as the MCE of DSHA.

4.3 MCE based on PSHA

Seismic source with magnitude (M_b) distribution of 83 events from 1963 to 2008 within the radius range of 500 km in Ulu Padas Area is as presented in Fig. 7a. It shows that

earthquake clusters are grouped in hypocentral distances of 200–300 km and 400–500 km. Very few earthquakes occur within the distance 0–100 km compared with the previous distance range. The western side of Ulu Padas Area appears to contribute seismicity more than the eastern side. The earthquake distribution in the site region is divided into two area sources, as shown in Fig. 7b. It has earthquakes with a minimum magnitude of M_{\min} 4 and a maximum magnitude of M_{\max} 6.2 for source 1 and M_{\max} 5.7 for source 2. Both area sources have low dense scattered distribution of seismicity. In this study, the effect of catalog completeness of earthquake event to the b -value of Gutenberg–Richter law is neglected. Area sources 1 and 2 have a Gutenberg–Richter constant of a - and b -values, namely 4.970 and 0.773, and 5.775 and 0.9805, respectively.

To accommodate the large dam effect in PSHA, we include RTS source using an area seismic source as discussed previously. The source has M_{\max} 4.5, which is based on predicted RTS, and assumed M_{\min} 4.0. Moreover, the study has assumed two M 4.1 as the additional events in order to get the b -value higher than the value in source 1 and 2. It was also aimed to reach the annual rate lower than other sources. Hence, 5.371 and 1.188 of a - and b -values were selected for RTS source, respectively. The annual rates of occurrence for earthquake magnitude M equal or more than M_{\min} , $k(M \geq M_{\min})$, for sources 1 and 2 are depicted in Fig. 7b. Based on the bounded exponential recurrence law, the annual rate of occurrence (k_m) for area seismic sources 1 and 2 within the hypocentral distance $R \leq 500$ km is found to be very close at 1.512 and 1.539, respectively (Fig. 9). This explains why the number of earthquake events for both area sources 1 and 2 is very close as well. RTS seismic source is estimated having 1.058 of annual rate within the hypocentral distance $R \leq 200$ km. In this study, no characteristic occurrence model was employed as the maximum magnitude in the area was less than 7.0. The annual rate of earthquake in the RTS seismic source has lower rate than other seismic sources.

Given that the PSHA was used to evaluate the seismic hazard of the site in Ulu Padas Area with and without a large dam effect, the analysis was performed twice. The disaggregation was conducted using bins of width 0.1 in magnitude, 10 km in hypocentral distance, and 0.2 in epsilon (ϵ). A number of scenarios are adopted for each case of PSHA to cover the epistemic uncertainty, as shown in the logic tree in Fig. 6, due to the lack of seismologic knowledge of the site. We assigned a 0.5 weight to the seismic sources 1 and 2 for the PSHA case without a large dam effect, and 0.4 for the PSHA case with a large dam effect. We set the weighted RTS seismic source to 0.2 because it has no record of seismicity, making it more uncertain than the other sources (Fig. 6). The maximum magnitude in the RTS seismic source was given a weight of 0.4 for M_b 4.5 and 0.6 for M_b 4.3 because the RTS M_b 4.5 is unlikely, as discussed in the previous section, and also to overcome the uncertainty of excessively increasing the hazard propagated by a short hypocentral distance (Fig. 6).

The total seismic hazard to the Ulu Padas Area is depicted in Fig. 10. This figure demonstrates the eleven selected attenuation models contributing to the total seismic hazard for the site as well. Although we weighted low, the Toro et al. (1997) model produces a superior PGA hazard to the site, while the Atkinson and Boore (2006) model is inferior to the others. Among the attenuation models, the Ambraseys et al. (2005) model that has the highest weight tends to underestimate and overestimate the PGA hazard significantly in frequent and rare earthquakes, respectively. This indicates that the Ambraseys' model produces a lower ground motion in a low-magnitude (or long-distance) earthquake and higher ground motion in a high-magnitude (or short-distance) earthquake than the other attenuation models.

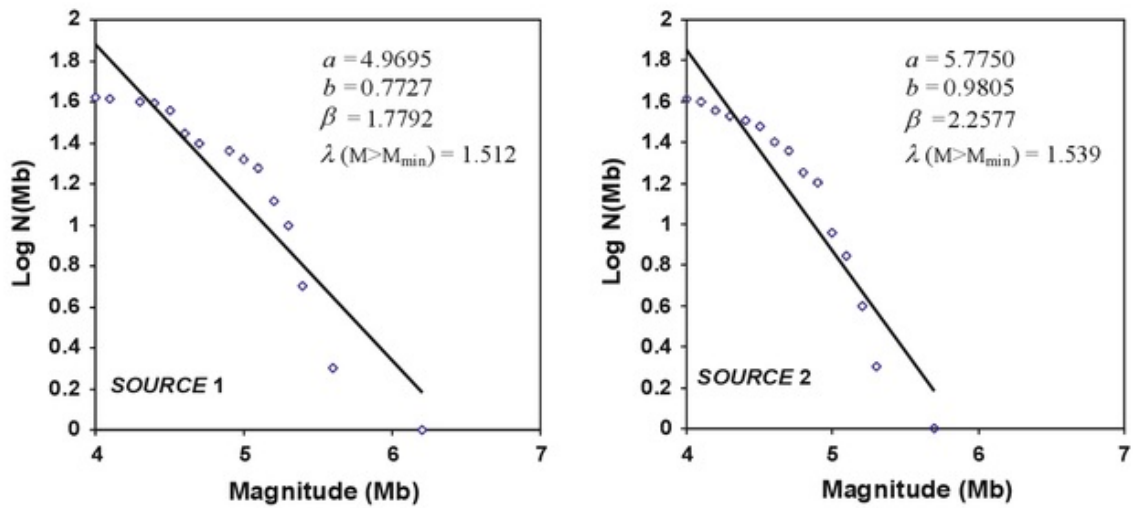


Fig. 9 Annual rate of occurrence for magnitude (M [Mb]) and Gutenberg–Richter parameters for seismic sources 1 and 2

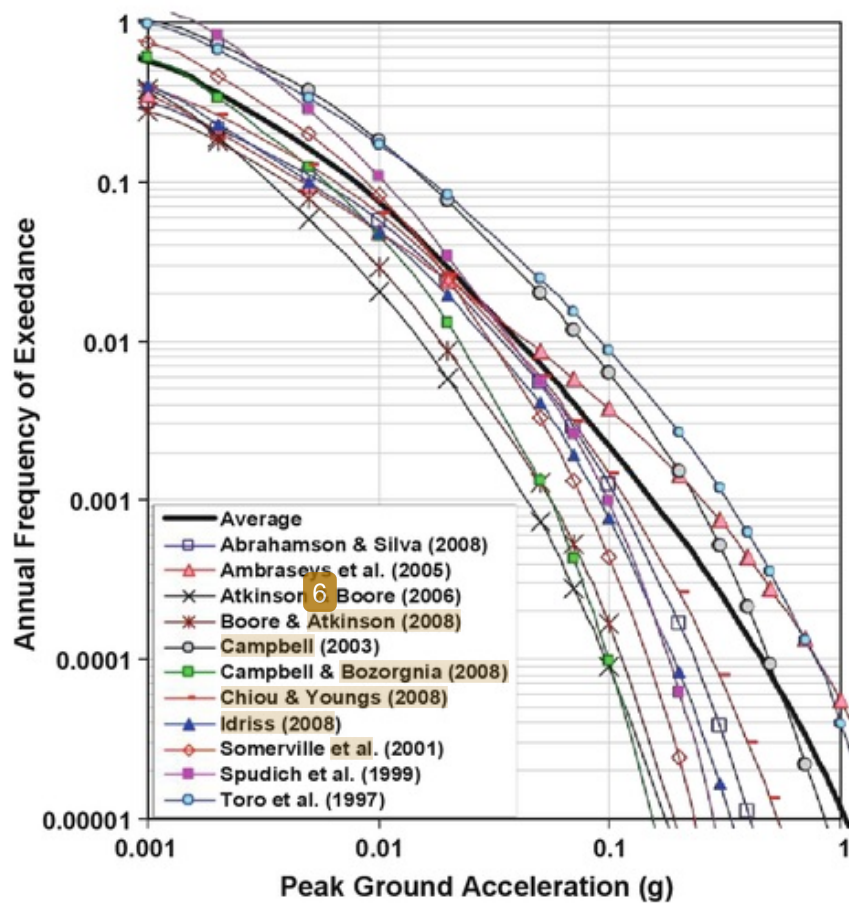


Fig. 10 Contributions of attenuation models to the total seismic hazard

Figure 11a and b describes the SA of the total hazard at the PGA and a 1.0-s period, respectively. The PGA with a 10% probability of occurrence within 50 years of a building life span (or an earthquake with a return period of 475 years) is 0.1026 g for the PSHA

with a large dam effect and 0.0354 g for the PSHA without a large dam effect. The result with a large dam effect is higher than that with the upper bound range of the Global Hazard Assessment Program, i.e., 0.040–0.080 g. The earthquake hazard in a 2,475 years RPE at the site may probably reach 0.2433 g if we include a large dam effect (RTS), which is significantly higher than 0.0694 g if the RTS analysis without a large dam effect is considered. In the SA at 1.0-s period, henceforth SA(1.0 s), the total hazard is nearly identical with the rare earthquakes for both PSHA cases. These results are listed in Table 6, including the percentage of contribution of each seismic source area to the total seismic hazard.

Although having a lower maximum magnitude, the seismic source 2 governs the total hazard in the short-period SA for the PSHA without a large dam effect, as clearly described in Table 6. On the contrary, the seismic source 1 controls the seismic hazard at the long-period SA, indicating that the hypocentral distance adds more hazard than the magnitude. This indication reveals that seismic sources 1 and 2 were not distorted although the RTS seismic source was introduced. The effect of a large dam is clearly presented in Table 6 and Fig. 11a, particularly in the short-period SA. The effect is not apparent at the long-period SA for the entire return periods of earthquake, which is replaced by the seismic source 1, as clearly shown in Fig. 11b. The trend is also demonstrated in the uniform hazard spectrum as illustrated in Fig. 12. The plot shows a sharp contrast in the effect of a large dam at a period of less than 1.0 s and then supersedes the SA hazard without a large dam effect, as represented by the coinciding lines, indicating that the distant earthquakes are dominant.

Table 7a and b presents joint magnitude–distance–epsilon (M – R – e) distributions resulting from the disaggregation of the 5% damped linear elastic SA values at periods of PGA, 0.1 s, and 1.0 s that correspond to 475 and 2,475 years RPEs for the investigated site in Ulu Padas Area with and without large dam effect. The listed values are mode and mean of joint distribution M – R – e . Herein, the mode values are the central values of the M , R , and e bins used in the calculations. The disaggregation of the 475 and 2,475 years PGA and SA(0.1 s) values show that the earthquakes of lower size occurring at shorter distances dominate the analysis without large dam effect. It means that as the RPE increases, the

Table 6 Spectrum acceleration on the bedrock based on the contribution of seismic sources to the total seismic hazard of the investigated site

Return period	Without dam		Return period With dam	
	2,475 years (2% in 50 years)	475 years (10% in 50 years)	2,475 years (2% in 50 years)	475 years (10% in 50 years)
<i>(a) Period of PGA</i>				
Source 1	0.0273 g (39.4%)	0.0143 g (40.4%)	Source 1	0.0027 g (1.1%) 0.0023 g (2.2%)
Source 2	0.0421 g (60.7%)	0.0211 g (59.6%)	Source 2	0.0039 g (1.6%) 0.0035 g (3.4%)
–	–	–	Source RTS	0.2374 g (97.3%) 0.0969 g (94.4%)
Total	0.0694 g	0.0354 g	Total	0.2440 g 0.1026 g
<i>(b) Period 1.0 s</i>				
Source 1	0.0273 g (76.8%)	0.0132 g (74.4%)	Source 1	0.0208 g (57.1%) 0.0101 g (54.1%)
Source 2	0.0083 g (23.2%)	0.0045 g (25.6%)	Source 2	0.0062 g (17.1%) 0.0034 g (18.2%)
–	–	–	Source RTS	0.0094 g (25.8%) 0.0052 g (27.7%)
Total	0.0356 g	0.0177 g	Total	0.0365 g 0.0186 g

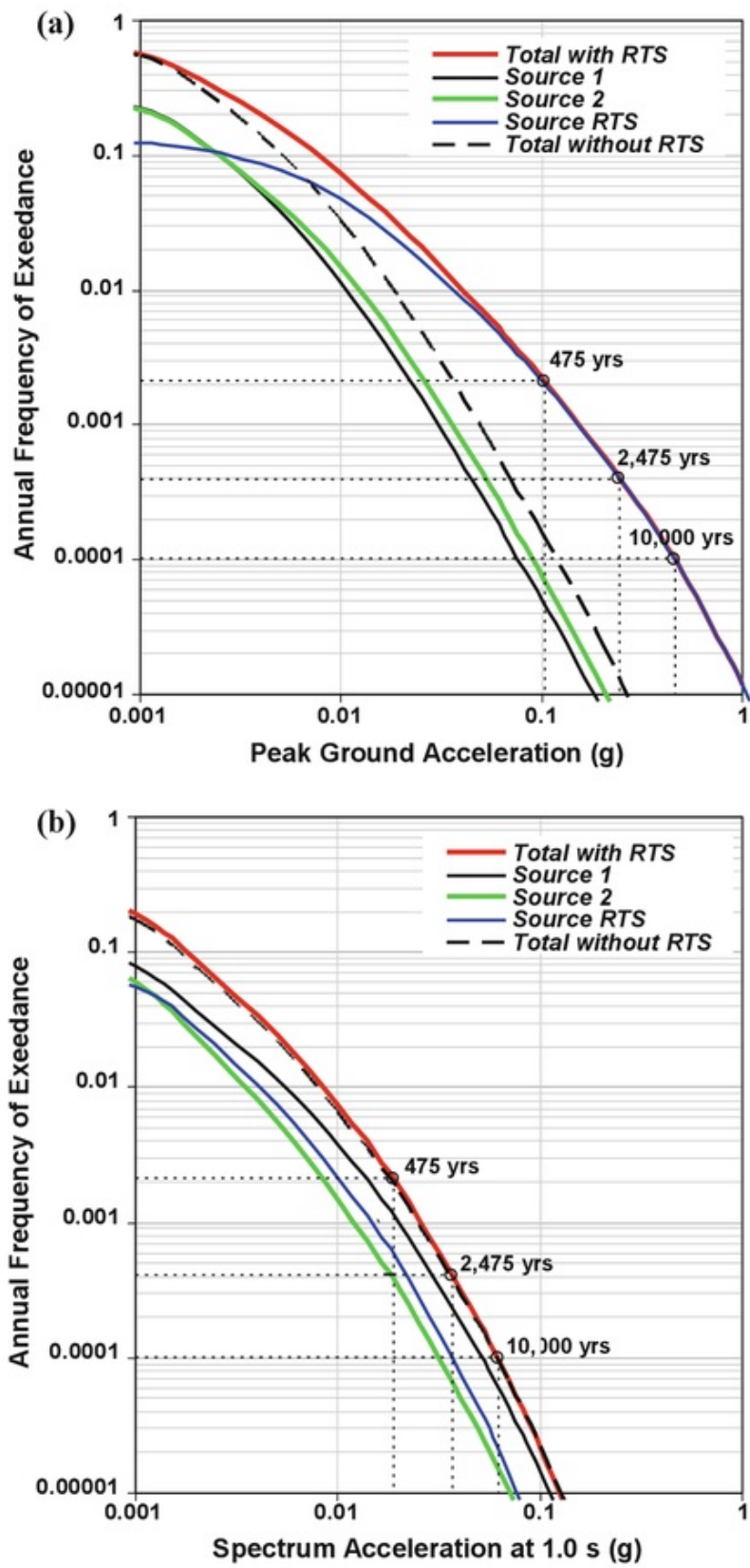


Fig. 11 Contribution of seismic sources to the total seismic hazard at period of PGA and 1.0 s

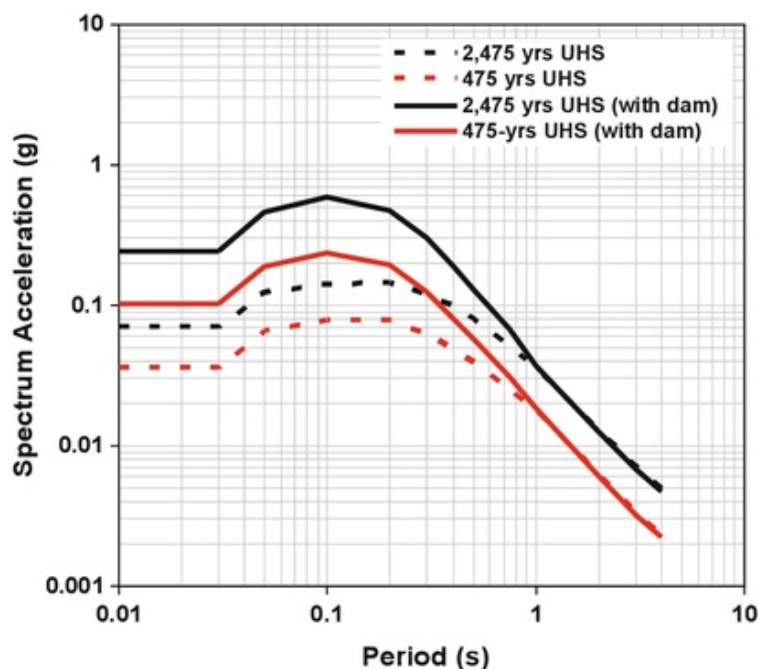


Fig. 12 Comparison of UHS for 2,475 and 475 years RPE with and without the effect of large dam at the investigated site

Table 7 Controlling earthquakes in tripled $M-R-e$ of 2,475 and 475 years RPEs at short and long periods of uniform hazard spectra (UHS) acceleration on the bedrock: (a) without large dam effect, (b) including large dam effect

(a)									
	PGA = 0.069 g		SA(0.1 s) = 0.140 g		SA(1.0 s) = 0.036 g				
2,475 Mode M	R = 130 km	e = 1.3	M 5.7	R = 90 km	e = 1.3	M 6.1	R = 190 km	e = 1.3	
	5.7								
Mean M	R = 130 km	e = 1.0	M 5.5	R = 120 km	e = 1.4	M 6.1	R = 200 km	e = 1.2	
	5.6								
	PGA = 0.035 g		SA(0.1 s) = 0.078 g		SA(1.0 s) = 0.018 g				
475 Mode M	R = 190 km	e = 0.9	M 5.7	R = 130 km	e = 1.1	M 6.1	R = 190 km	e = 1.5	
	5.7								
Mean M	R = 140 km	e = 0.9	M 5.7	R = 130 km	e = 1.1	M 6.2	R = 200 km	e = 1.4	
	5.5								
(b)									
	PGA = 0.244 g		SA(0.1 s) = 0.588 g		SA(1.0 s) = 0.037 g				
2,475 Mode M	R = 10 km	e = 0.7	M 4.3	R = 10 km	e = 0.5	M 6.1	R = 190 km	e = 1.5	
	4.3								
Mean M	R = 19 km	e = 1.0	M 4.3	R = 17 km	e = 1.1	M 5.7	R = 160 km	e = 1.3	
	4.3								
	PGA = 0.103 g		SA(0.1 s) = 0.236 g		SA(1.0 s) = 0.019 g				
475 Mode M	R = 12 km	e = 0.3	M 4.3	R = 12 km	e = 0.4	M 6.1	R = 190 km	e = 0.7	
	4.3								
Mean M	R = 26 km	e = 0.6	M 4.3	R = 24 km	e = 0.7	M 5.7	R = 160 km	e = 1.0	
	4.4								

controlling earthquakes become slightly greater in M and occur closer to the investigated site. However, this is not the case for M – R of SA(1.0 s), which tends to be equal for 475 and 2,475 years RPEs (Table 7b).

The disaggregations are also depicted in the joint distribution graph of M – R for the 2,475 years RPE shown in Fig. 13. The disaggregation plot of the 475 years RPE is not presented because it has an identical trend with the former earthquake. Figure 13a shows that the 2,475 years SA hazard without a large dam at a period of PGA is controlled by distant earthquakes (from 90 to 190 km) of low to strong magnitude (from M 4.9 to M 6.3). Larger earthquakes and distant events dominated the SA(1.0 s) value for the same return period. This indicates that the predicted RTS triggered by the future large dam would affect the joint distribution M – R of total hazard at the site in the Ulu Padas Area, particularly at short-period SA, which is dominated by the lower magnitudes and shorter hypocentral distances, as indicated in Fig. 13b.

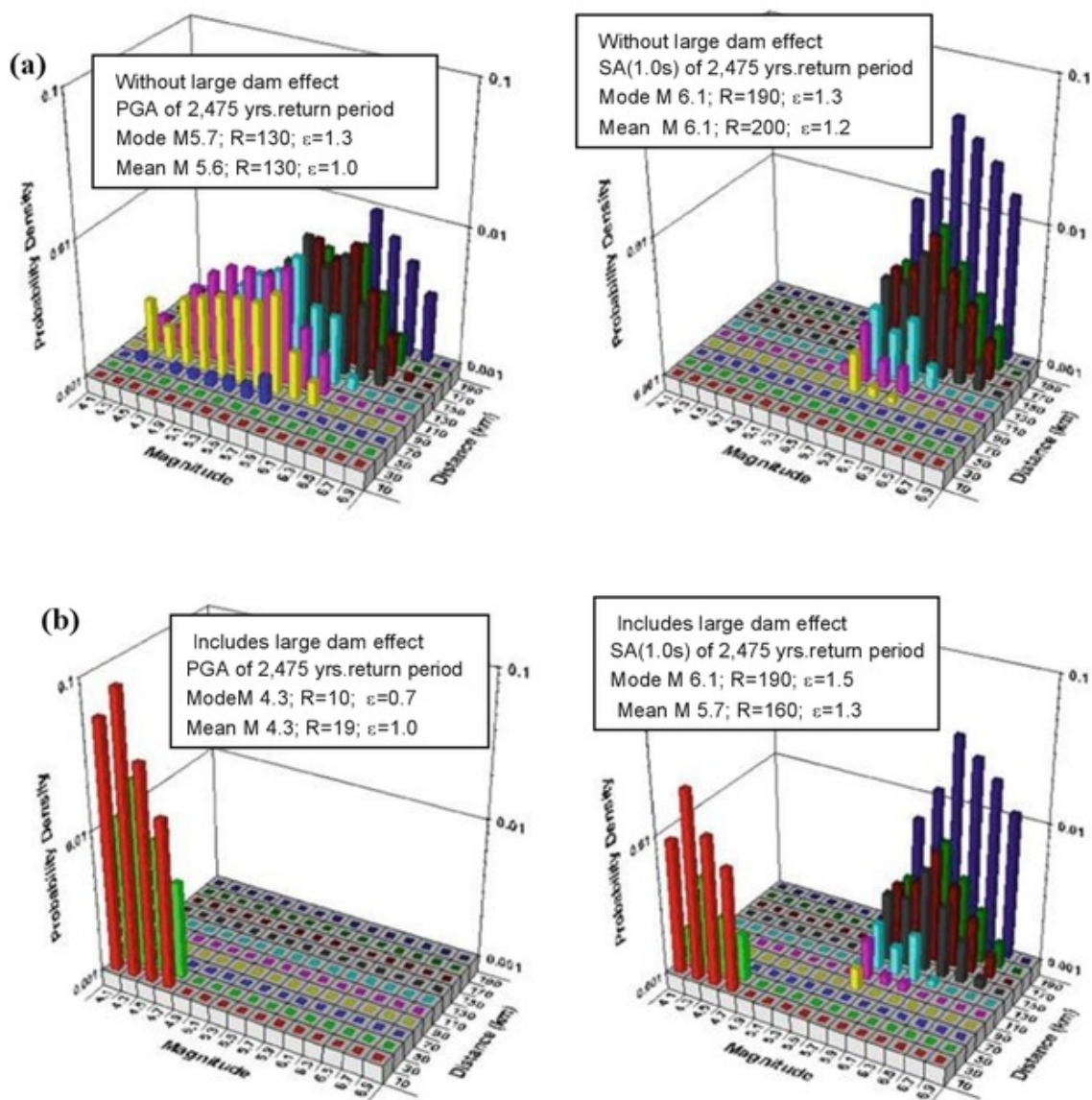


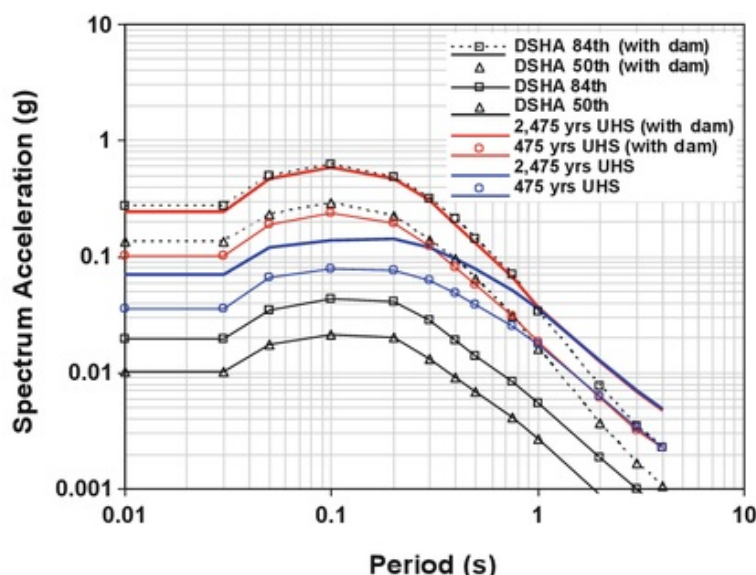
Fig. 13 Disaggregation of seismic hazard for magnitude–distance (M – R) at period of PGA and 1.0 s: a without large dam effect, b includes large dam effect

Analyzing mode e behavior with SA period for 2,475 years RPE does not explain any particular trend. That is, both values of mode and mean e from the analysis with and without large dam neither increase nor decrease regularly with increasing spectral period. Unlike the mode and mean values of e from PSHA with large dam, mode and mean values of e from the PSHA without large dam tend to increase as the return period of earthquake increases. For instance, the mean values of e is in the range of 0.6–1.0, where the e range means that the dominant ground motions are within $0.4r$ of the median for a 475 years RPE, whereas the 2,475 years RPE is in the range of 1.0–1.3. Hence, we can conclude that the effect of RTS of a large dam probably distorts the increasing trend of mode and mean values of e . For the 475 years RPE, the local event contributing the most to the SA hazard with a large dam effect at the PGA period corresponds to the mode scenario, M 4.3, $R = 12$ km, and $e = 0.3$, whereas the 2,475 years RPE corresponds to a slightly shorter distance mode scenario, M 4.3, $R = 10$ km, and $e = 0.7$. The contribution of the regional earthquake to the SA hazard at a period of 1.0 s for both cases is mainly associated with the mode and mean scenarios having magnitudes of 5.7–6.2 at distances between 160 and 200 km.

4.4 Effect of large dam on the maximum design earthquake

We compared the MCEs from the PSHA (SA in Table 7) and DSHA (Table 5) to define the MDE (McGuire 2001). For brevity, the SA of the governed MCE are presented in one graph, as shown in Fig. 14, indicating that the SA at the PGA period are generally similar to the DSHA with a large dam at the 84th-percentile and the 2,475 years RPE, i.e., 0.2727 g and 0.2440, respectively. The trend is the same for SA at a longer period of up to 1.0 s. This indicates that the predicted RTS earthquake, M_b 4.5 and $R = 10.4$ km, will probably occur at a return period longer than 2,475 years or have more than 2.0% of the probability of exceedance within a 50-year building life span. Without a large dam, the DSHA controlling earthquake, M_b 4.5 and $R = 55$ km, seems to be more frequent than the 475 years earthquake, M_w 4.3 and $R = 12$ km. This earthquake trend tends to occur rarely at more than 1.0 s of the SA period when compared with the seismic hazard that considers a large dam effect. The median SA, or the 50th-percentile, has a similar pattern to the SA at the 84th-percentile, using the 475 years earthquake as the point of comparison. The median

Fig. 14 Comparison of spectrum acceleration of UHS and DSHA at 84th- and 50th-percentiles with and without the effect of large dam

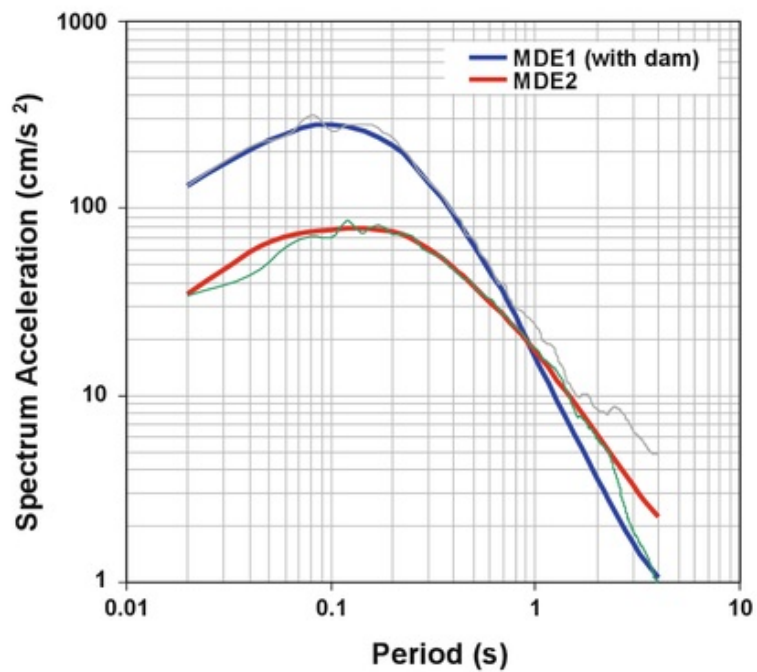


SA of DSHA probably has a RPE of between 475 and 2,475 years. The analysis without a large dam gives the PGA range of 0.022–0.034 g for the 475 and 2,475 years earthquakes, respectively. In contrast, it is almost twice as high as the 84th-percentile DSHA at a range of 0.006–0.020 g.

The effect of a large dam is significantly apparent in the selection of MCE as the MDE. Without a large dam, the seismic hazard at a site is governed by the MCE from the 2,475 and 475 years RPEs, which adversely poses a seismic hazard for a site that may have a large dam in the future. In this case, the MCE earthquakes at the 84th- and 50th-percentiles of the DSHA control the seismic hazard. Nevertheless, both conditions of having and without a large dam need to be considered in the selection of the MDE for regular structures, e.g., apartment, offices, school, and bridges because the seismic hazard at a longer period SA (i.e., more than 1.0 s) governs the seismic hazard without a large dam or distant earthquakes. Based on this condition, the MDE is selected from the MCE of DSHA at the median for the SA at a period of less than 1.0 s, whereas the SA of the 475 years RPE is selected for the MDE at a period of more than 1.0 s, as illustrated in Fig. 15. This MDE governs the seismic hazard, regardless of the presence of a large dam.

In most assessments of moderate to high seismic hazard regions, MCE value based on Wells and Coppersmith (1994) or Hanks and Bakun (2002) empirical relationships (DSHA) is superior compared with the PSHA results and earthquake due to RTS (having a large dam). However, these are not absolute conditions for all of seismic hazard analysis cases, as discussed in the previous section. For a low seismic and stable region, especially the region with very insufficient active fault data (no data of slip rate and rupture length/width/area), the case of MDE may be posed differently (McGarr et al. 2002; Wieland 2004; ICOLD 2004), such as at the investigated site in Ulu Padas Area of Northern Borneo region as demonstrated in this study.

Fig. 15 Spectrum accelerations of MDE and mean matched-spectrum accelerations of selected ground motions for the investigated site



4.5 Effect of the large dam on the selection of ground motion

We selected the ground motion records from ISESD (Ambraseys et al. 2001) and PEER (2000) to represent the seismic regions with and without a large dam, as shown in Table 8. The selection was based on the seismologic source parameters, namely magnitude (4.0–6.0), hypocentral distance (40–160 km), sedimentary rock or general rock site condition with shear wave velocity ranging from 600–800 m/s, and normal or reverse style-of-faulting. All selected time history accelerations were recorded from six earthquake events sourced from California, USA, Turkey, Italy, and Greece. There was no strong motion record that could represent the normal or reverse mechanism of distant earthquakes $M \leq 5$ and distance $R \leq 100$ km. It is obvious since the available records are mostly sourced from strong motion-type equipment that can be triggered for recording only by a strong-enough ground movement. This kind of weak tremor is hard to find at a rock site condition, especially when the motion sourced from the distant earthquake has a magnitude of less than 5.

Figure 16 shows the time history accelerations of the selected strong motions after they were spectrum-matched to the MDE SA. The matched-motion sourced from the distant earthquake to represent the earthquake motion sourced from the area with no large dam is shown on the left-hand side column (Fig. 16a). The RTS earthquake is represented by a suite of matched-motions on the right-hand side (Fig. 16b). The number at the top right-hand corner of each plot indicates the sequence number in Table 8. The figure clearly

Table 8 Selected ground motion records for the investigated site

No.	Data from/ earthquake name	Recorded station	Date	PGA (g)	M	R (km)	Dur. (s)	Style-of- faulting
<i>(a) Distant earthquakes represent earthquakes in current condition</i>								
1	ESD/Izmit (aftershock)	LDEO D0531 (EW)	11/11/99	0.0376	Mw 5.6	52.0	13.48	Reverse
2	ESD/Izmit (aftershock)	LDEO D0531 (NS)	11/11/99	0.0298	Mw 5.6	52.0	13.48	Reverse
3	PEER/Whittier Narrows	Malibu/A-MAL180	01/10/87	0.0480	Ms 5.7	65.3	18.83	Reverse
4	PEER/Whittier Narrows	Vasquez Rocks Park/ A-VAS90	01/10/87	0.0598	Ms 5.7	52.4	11.35	Reverse
5	PEER/Whittier Narrows	Vasquez Rocks Park/ A-VAS00	01/10/87	0.0600	Ms 5.7	52.4	11.56	Reverse
<i>(b) Near-field low-magnitude earthquakes represent RTS earthquakes</i>								
6	ESD/Friuli	Breginj-Fabrika IGLI (WE)	18/04/79	0.0387	Mw 4.6	16	3.74	Reverse
7	ESD/Friuli	Breginj-Fabrika IGLI (NS)	18/04/79	0.0852	Mw 4.6	16	2.98	Reverse
8	ESD/Gulf of Corinth (aftersh.)	Aigio-Military Factory (Trans)	22/02/97	0.0386	Mw 4.2	13	5.69	Normal
9	PEER/Anza (Horse Canyon)	Pinyot Flat 5044 (PFT045)	25/02/80	0.1100	Mw 4.9	12.0	3.27	Normal
10	PEER/Anza (Horse Canyon)	Pinyot Flat 5044 (PFT135)	25/02/80	0.1310	Mw 4.9	12.0	2.17	Normal

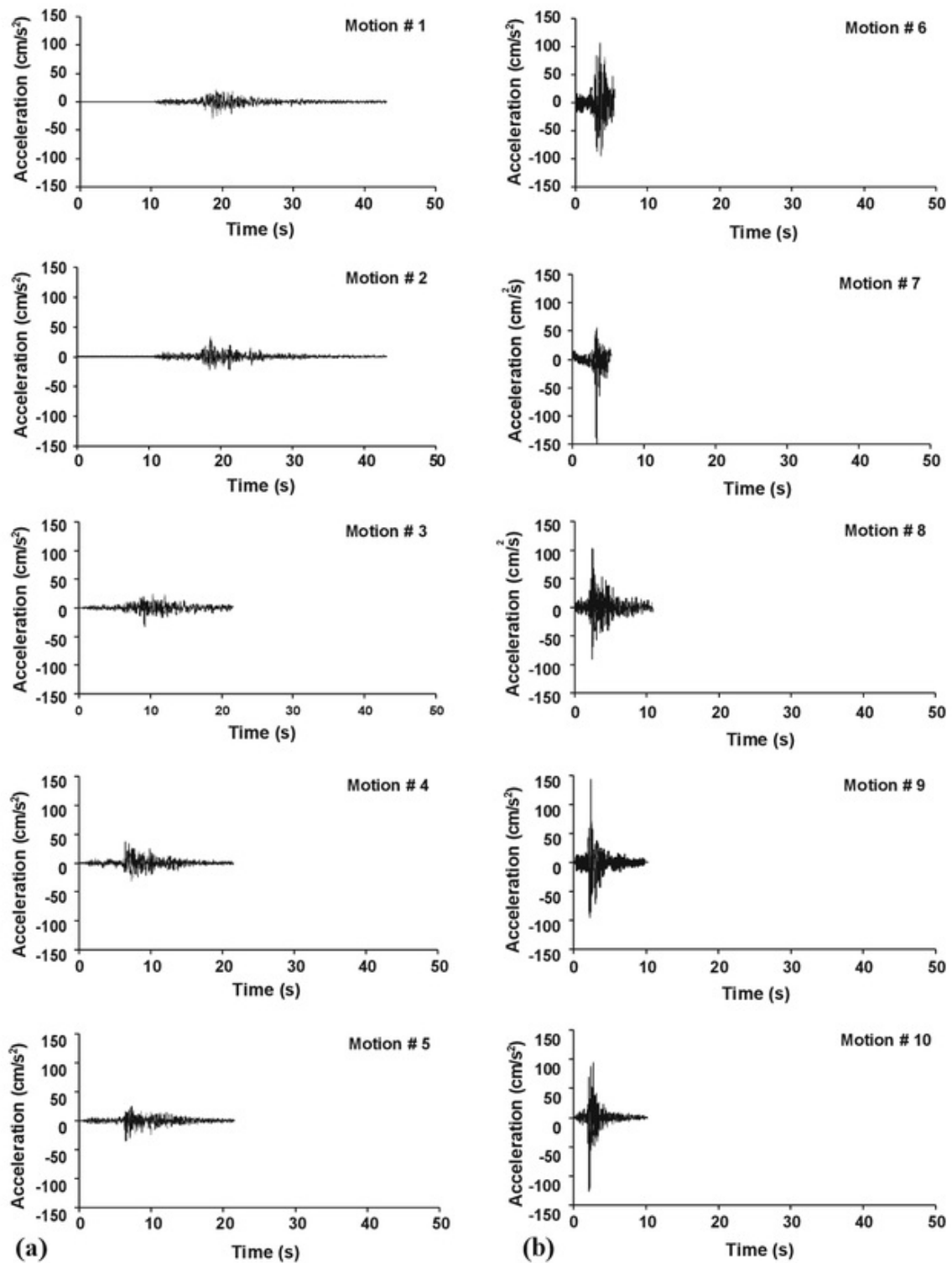


Fig. 16 Selected ground motions for the investigated site after MDE spectrum-matched: a for condition with no large dam, b for condition with large dam

indicates that the near-field motion has a shorter duration and a higher amplitude than the distant motion, as listed in Table 8. In this case, the near-field low-magnitude earthquakes only converged with the MDE spectra using the matched-spectrum method at an average period lower than 0.7 s, whereas a distant earthquake converged with the spectra at a

period of up to 2.0 s. This indicates that a near-field low-magnitude earthquake has rich higher frequency than a distant earthquake.

In structural engineering, particularly for flexible structures (defined as those having a fundamental period greater than 1.0 s), the effect of a large dam on the seismic hazard may not be apparent compared with the condition without a large dam. This shows that the existing rigid structures (buildings with a fundamental period lesser than 1.0 s) at the site are those that will be very vulnerable if a large dam will be constructed close to the active fault, because most of these structures were built based on the gravity load design using the British Standard. The regular brick-masonry houses, which are normally non-engineered constructions, are especially vulnerable. The seismic hazard discussed in this study is PGA on the bedrock (or rock) that does not include the local site effect. The local site effect may increase the PGA because of the soil effect, surface topography effect, and basin effect. For instance, the local soil at the site may amplify the motion up to 1.6 times the PGA on the bedrock according to Eurocode 8, and the crest of a ridge may amplify the average acceleration of about 2.5 times the average base acceleration (Kramer 1996). These are clearly not good signs for a regular building at the investigated site.

5 Conclusion

This study addressed the issue of whether any escalation of the seismic hazard could transpire in a low seismic region where a large dam may be constructed in the future. The seismic hazard is dedicated to a seismic design and assessment of a regular building at the site. The Ulu Padas Area in Northern Borneo is selected as a low seismic region that has a documented absence of earthquake history. We ran PSHA and DSHA in accordance with the RTS analysis to define the MCE and then determined the MDE. The large dam is assumed to have a water volume of 700–1,000 $\times 10^6$ m³ with a water level height of 120 m.

The surrounding Ulu Padas Area can be classified as a background seismic source area and can be divided into two source areas, namely source areas 1 and 2. These seismic sources propagate tremors on the site bedrock with a PGA ranging from 0.0029 to 0.0102 g based on the DSHA result at the median or 50th-percentile in their earthquake histories and are associated with low to moderate earthquake events, Mb 4.1–5.4, with 55–159 km hypocentral distances. The composite model from 11 ground motion models is employed in this case. The seismic hazard in the Ulu Padas Area, particularly in the investigated site, may increase to about 13 times based on the DSHA when a large dam is built near the fault line due to a predicted Mb 4.5 earthquake at a hypocentral distance of 10.4 km sourced from the RTS phenomenon. In the 84th-percentile of the DSHA or considering the worst case scenario, the reservoir could trigger a PGA of 0.2727 g on the bedrock of the investigated site.

Based on the PSHA, the seismic source areas 1 and 2 in the surrounding Ulu Padas Area have 0.773 and 0.9805 *b*-values of the Gutenberg–Richter constant, respectively, whereas the *b*-value of the RTS source is assumed to be 1.188. The annual rate of occurrence for source areas 1 and 2 is very close to each other and are higher than that of the RTS source. Based on the regional earthquake history, the maximum magnitude for source areas 1 and 2 and the RTS source are 6.2, 5.7, and 4.5, respectively, whereas the minimum magnitude is 4.0 for all sources. The analysis reveals that a 475 years RPE could produce 0.0354 g of PGA on the bedrock in the current seismic hazard level and could be increased to 2.9 times when propagated by an RTS earthquake when a future large dam is built. However, the

effect of a large dam on the seismic hazard may not be visible at periods of SA longer than 1.0 s. As the consequence, the MDE can be affected significantly by the future existence of a large dam. Therefore, the SA of the MDE for a regular building with a period of less than 1.0 s must be taken from the median value of the DSHA. Moreover, the SA of a 475 years RPE from the current condition (without a large dam effect) must also be considered as the MDE, particularly at SA periods of more than 1.0 s. Consequently, this affects the selection of the ground motion for the seismic design and assessment of regular buildings.

Acknowledgments Authors wish to acknowledge the financial support given by Universiti Sains Malaysia through the Zamalah Fellowship and the Universiti Sains Malaysia Research University Postgraduate Research Grant Scheme during the study. In this study, some helpful efforts in providing articles by Dr. Martin Wieland and supporting data by Ranhill Sdn. Bhd. are acknowledged. The authors would also like to thank the two anonymous referees for their valuable comments in the earlier version of this paper.

References

- Abrahamson NA (1992) Non-stationary spectral matching. *Seismol Res Lett* 63:30
- Abrahamson NA (2006) Seismic hazard assessment: problem with current practice and future development. In: *Proceeding of the 1st European conference on earthquake engineering and seismology, Geneva, Switzerland, 3–8 September 2006, Paper No: K2*
- Abrahamson NA, Silva WJ (2008) Summary of the Abrahamson & Silva NGA ground motion relations. *Earthq Spectr* 24:67–97
- Ambraseys N, Smit P, Sigbjörnsson R, Suhadolc P, Margaris B (2001) Internet-site for European strong-motion data. <http://www.isesd.cv.ic.ac.uk>, EVR1-CT-1999-40008, European Commission, Directorate-General XII, Environmental and Climate Programme, Bruxelles, Belgium
- Ambraseys NN, Douglas J, Sarma SK, Smit PM (2005) Equations for the estimation of strong ground motions from shallow crustal earthquakes using data from Europe and the Middle East: horizontal peak ground acceleration and spectral acceleration. *Bull Earthq Eng* 3:1–53
- Anbazhagan P, Vinod JS, Sitharam TG (2009) Probabilistic seismic hazard analysis for Bangalore. *Nat Hazards* 48:145–166
- ASCE (2007) ASCE/SEI Standard 41–06, Seismic rehabilitation of existing buildings (including Supplement 1). American Society of Civil Engineers, Reston
- Atakan K, Midzi V, Moreno Toiran B, Vanneste K, Camelbeeck T, Meghraoui M (2000) Seismic hazard in regions of present day low seismic activity: uncertainties in the paleoseismic investigations along the Bree Fault Scarp (Roer Graben, Belgium). *Soil Dyn Earthq Eng* 20:415–427
- Atkinson GM, Boore DM (2006) Earthquake ground-motion prediction equations for eastern North America. *Bull Seismol Soc Am* 96:2181–2205
- Baecher BG, Keeney RL (1982) Statistical examination of reservoir induced seismicity. *Bull Seismol Soc Am* 72:553–569
- Balendra T, Lam NTK, Wilson JL, Hong KH (2002) Analysis of long-distance earthquake tremors and base shear demand for buildings in Singapore. *Eng Struct* 24:99–108
- Bazzurro P, Cornell CA (1999) Disaggregation of seismic hazard. *Bull Seismol Soc Am* 89:501–520
- Bolt BA, Cloud WK (1974) Recorded strong motion on the Hsinfengkiang Dam, China. *Bull Seismol Soc Am* 64:1337–1342
- Bommer JJ, Acevedo A (2004) The use of real earthquake accelerograms as input to dynamic analysis. *J Earthq Eng* 8:43–91
- Bommer JJ, Martinez-Pereira A (1999) The effective duration of earthquake strong motion. *J Earthq Eng* 3:127–172
- Boore DM, Atkinson GM (2008) Ground-motion prediction equations for the average horizontal component of PGA, PGV, and 5%-damped PSA at spectral periods between 0.01 s and 10.0 s. *Earthq Spectr* 24:99–138
- BSSC (2001) NEHRP recommended provisions for seismic regulations for new buildings and other structures 2000 Edition, part 1- provisions (FEMA 368). Building Seismic Safety Council, Washington, DC
- Campbell KW (2003) Prediction of strong ground motion using the hybrid empirical method and its use in the development of ground motion (attenuation) relations in eastern North America. *Bull Seismol Soc Am* 93:1012–1033

- Campbell KW, Bozorgnia Y (2008) NGA ground motion model for the geometric mean horizontal component of PGA, PGV, PGD and 5% damped linear elastic response spectra for periods ranging from 0.01 to 10 s. *Earthq Spectr* 24:139–171
- CEN (2004) European standard EN 1998-1:2004 Eurocode 8: design of structures for earthquake resistance, part 1: general rules, seismic actions and rules for buildings. Comité Européen de Normalisation, Brussels
- Chadha RK, Gupta HK, Kumpel HJ, Mandal P, Rao AN, Sarin N, Radhakrishna I, Rastogi BK, Raju IP, Sarma CSP, Satyamurthy C, Satyanarayana HVS (1997) Delineation of active faults, nucleation process and pore pressure measurements at Koyna (India). *Pure Appl Geophys* 150:551–562
- Chiou BSJ, Youngs RR (2008) Chiou-Youngs NGA ground motion relations for the geometric mean horizontal component of peak and spectral ground motion parameters. *Earthq Spectr* 24:173–215
- Cotton F, Scherbaum F, Bommer JJ, Bungum H (2006) Criteria for selecting and adjusting ground-motion models for specific target applications: applications to Central Europe and rock sites. *J Seismol* 10:137–156
- Dobry R, Idriss IM, Ng E (1978) Duration characteristics of horizontal components of strong-motion earthquake records. *Bull Seismol Soc Am* 68:1487–1520
- Douglas J (2003) Earthquake ground motion estimation using strong-motion records: a review of equations for the estimation of peak ground acceleration and response spectral ordinates. *Earth-Sci Rev* 61:43–104
- Douglas J, Aochi H (2008) A survey of techniques for predicting earthquake ground motions for engineering purposes. *Surv Geophys* 29:187–220
- FEMA (2005) Federal guidelines for dam safety: earthquake analyses and design of dams. FEMA 65. Building Seismic Safety Council, Washington, DC
- Gupta HK (2002) A review of recent studies of triggered earthquakes by artificial water reservoirs with special emphasis on earthquakes in Koyna, India. *Earth-Sci Rev* 58:279–310
- Gutenberg B, Richter CF (1944) Frequency of earthquakes in California. *Bull Seismol Soc Am* 34:185–188
- Han S-W, Choi Y-S (2007) Seismic hazard analysis in low and moderate seismic region-Korean peninsula. *Struct Saf* 30:543–558
- Hancock J, Watson-Lamprey J, Abrahamson NA, Bommer JJ, Markatis A, McCoy E, Mendis R (2006) An improved method of matching response spectra of recorded earthquake ground motion using wavelets. *J Earthq Eng* 10:67–89
- Hanks TC, Bakun WH (2002) A bilinear source-scaling model for M–log A observations of continental earthquakes. *Bull Seismol Soc Am* 92:1841–1846
- ICOLD (1983) Seismicity and dam design. Bulletin 46, International Commission on Large Dams
- ICOLD (1989) Selecting seismic parameters for large dams—guidelines and recommendations. Bulletin 72, International Commission on Large Dams
- ICOLD (2004) Reservoir and seismicity: state of knowledge. Bulletin 137, International Commission on Large Dams
- Idriss IM (2008) An NGA empirical model for estimating the horizontal spectral values generated by shallow crustal earthquakes. *Earthq Spectr* 24:217–242
- JMGM (2006) Study on the seismic and tsunami hazards and risks in Malaysia. Report on the geological and seismic information of Malaysia submitted to ASM (unpublished)
- Kramer SL (1996) *Geotechnical earthquake engineering*. Prentice-Hall, Upper Saddle River
- Krinitzsky EL (1995) Deterministic versus probabilistic seismic hazard analysis for critical structures. *Eng Geol* 40:1–7
- Krinitzsky EL (2002) How to obtain earthquake ground motions for engineering design. *Eng Geol* 65:1–16
- Lantada N, Irizarry J, Barbat AH, Goula X (2010) Seismic hazard and risk scenarios for Barcelona, Spain, using the Risk-UE vulnerability index method. *Bull Earthq Eng* 8:201–229
- Levdecker G, Kopera JR (1999) Seismological hazard assessment for a site in Northern Germany, an area of low seismicity. *Eng Geol* 52:293–304
- McGarr A, Simpson D, Seeber L (2002) Case history of induced and triggered seismicity. In: Lee WHK, Kanamori H, Jennings PC, Kisslinger C (eds) *International handbook of earthquake and engineering seismology*, 4th edn. Academic Press, Amsterdam, pp 647–661
- McGuire RK (2001) Deterministic vs. probabilistic earthquake hazards and risks. *Soil Dyn Earthq Eng* 21:377–384
- McGuire RK (2004) *Seismic hazard and risk analysis*. Earthquake Engineering Research Institute, Berkeley
- Meng LK (1999) Geological setting of Sabah. In: *The petroleum geology and resources of Malaysia*, Petroleum Nasional Berhad (PETRONAS), Kuala Lumpur
- Michell GW, Becker M, Angermann D, Reigber C, Reinhart E (2000) Crustal motion in E- and SE-Asia from GPS measurements. *Earth Planets Sp* 52:713–720

- NEIC (2007) Earthquake database. National Earthquake Information Center. Available at <http://neic.usgs.gov/neic/epic>
- Ornthammarath T, Wamitchai P, Worakanchana K, Zaman S, Sigbjornsson R, Lai CG (2010) Probabilistic seismic hazard assessment for Thailand. *Bull Earthq Eng*. doi:10.1007/s10518-010-9197-3
- PEER (2000) PEER strong motion database. Available at: <http://peer.berkeley.edu/smcat/>
- Petersen MD, Dewey J, Hartzell S, Mueller C, Harmsen S, Frankel AD, Rukstales K (2004) Probabilistic seismic hazard analysis for Sumatra, Indonesia and across the Southern Malaysian Peninsula. *Tectonophysics* 390:141–158
- Reiter L (1990) *Earthquake hazard analysis: issues and insights*. Columbia University Press, New York
- RiskEngineering Inc (2008) EZ-FRISK™ version 7.3, software for earthquake ground motion estimation: user manual, Boulder, Colorado
- Sabetta F, Lucantoni A, Bungum H, Bommer JJ (2005) Sensitivity of PSHA results to ground-motion prediction relations and logic-tree weights. *Soil Dyn Earthq Eng* 25:317–329
- Scherbaum F, Bommer JJ, Bungum H, Cotton F, Abrahamson NA (2005) Composite ground-motion models and logic trees: methodology, sensitivities, and uncertainties. *Bull Seismol Soc Am* 95:1573–1593
- Seismosoft (2009) SeismoMatch vers 1.0.2. Available at: <http://www.seismosoft.com/>
- Simpson DW, Leith WS, Scholz CH (1988) Two types of reservoir-induced seismicity. *Bull Seismol Soc Am* 78:2025–2040
- Somerville P, Collins N, Abrahamson N, Graves R, Saikia C (2001) Ground motion attenuation relations for the central and eastern United States. US Geological Survey, Award 99HQGR0098 final report
- Spudich P, Joyner WB, Lindh AG, Boore DM, Margaris BM, Fletcher JB (1999) SEA99: a revised ground motion prediction relation for use in extensional tectonic regimes. *Bull Seismol Soc Am* 89:1156–1170
- Iwani P (1997) On the nature of reservoir-induced seismicity. *Pure Appl Geophys* 150:473–492
- Tongkul F (1993) Tectonic control on the development of the Neogene basins in Sabah, Malaysia. *Geol Soc Malays Bull* 33:95–103
- Tongkul F (1997) Polyphase deformation in the Telupid area, Sabah, Malaysia. *J Asian Earth Sci* 15:175–183
- Tongkul F (1999) Regional geological correlation of Paleogene sedimentary rocks between Sabah and Sarawak. *Geol Soc Malays Bull* 43:31–39
- Tongkul F (2006) The structural style of Lower Miocene sedimentary rocks, Kudat Peninsula, Sabah. *Geol Soc Malays Bull* 49:119–124
- Toro GR, Abrahamson NA, Schneider JF (1997) Models of strong ground motions from earthquakes in central and eastern North America: best estimates and uncertainties. *Seismol Res Lett* 68:41–57
- ICOLD (1997) Reservoir triggered seismicity. United States Committee on Large Dams, Report
- Utsu T (2002) Relationships between magnitude scales. In: Lee WHK, Kanamori H, Jennings PC, Kisslinger C (eds) *International handbook of earthquake and engineering seismology*, 81st edn. Academic Press, Amsterdam, pp 733–746
- Walpersdorf A, Vigny C, Subarya C, Manurung P (1998) Monitoring of the Palu-Koro fault (Sulawesi) by GPS. *Geophys Res Lett* 25:2313–2316
- Wells DL, Coppersmith KJ (1994) New empirical relationships among magnitude, rupture length, rupture width, rupture area, and surface displacement. *Bull Seismol Soc Am* 84:974–1002
- Wieland M (2004) *Earthquake safety of concrete dams and seismic design criteria for major dam projects*. ICOLD publication
- Wieland M (2005) Review of seismic design criteria of large concrete and embankment dams. In: *Proceeding of 73rd Annual Meeting of ICOLD*, Tehran, Iran, 1–6 May, 2005
- Wiemer S, Giardini D, Fäh D, Deichmann N, Sellami S (2009) Probabilistic seismic hazard assessment of Switzerland: best estimates and uncertainties. *J Seismol* 13:449–478

ORIGINALITY REPORT

11 %	%	%	11 %
SIMILARITY INDEX	INTERNET SOURCES	PUBLICATIONS	STUDENT PAPERS

PRIMARY SOURCES

1	Submitted to Indian Institute of Science, Bangalore Student Paper	1 %
2	Submitted to University of Brighton Student Paper	1 %
3	Submitted to Universiti Teknologi Petronas Student Paper	1 %
4	Submitted to National Institute of Technology, Rourkela Student Paper	<1 %
5	Submitted to Swinburne University of Technology Student Paper	<1 %
6	Submitted to Middle East Technical University Student Paper	<1 %
7	Submitted to Higher Education Commission Pakistan Student Paper	<1 %
8	Submitted to University of Melbourne Student Paper	<1 %
9	Submitted to University of Malaya Student Paper	<1 %
10	Submitted to Universiti Sains Malaysia Student Paper	<1 %
11	Submitted to University of Leeds Student Paper	<1 %

12	Submitted to De La Salle University - Manila Student Paper	<1%
13	Submitted to University of Nevada Reno Student Paper	<1%
14	Submitted to Asian Institute of Technology Student Paper	<1%
15	Submitted to University of Edinburgh Student Paper	<1%
16	Submitted to SDMI Student Paper	<1%
17	Submitted to Rochester Institute of Technology Student Paper	<1%
18	Submitted to University of Glasgow Student Paper	<1%
19	Submitted to Chulalongkorn University Student Paper	<1%
20	Submitted to King Fahd University for Petroleum and Minerals Student Paper	<1%
21	Submitted to Universiti Tenaga Nasional Student Paper	<1%
22	Submitted to Wright State University Student Paper	<1%
23	Submitted to Universiti Teknologi MARA Student Paper	<1%
24	Submitted to University of Portsmouth Student Paper	<1%
25	Submitted to University of Wollongong Student Paper	<1%
26	Submitted to Universiti Kebangsaan Malaysia Student Paper	<1%

27	Submitted to Indian Institute of Technology Student Paper	<1%
28	Submitted to Indian Institute of Technology Guwahati Student Paper	<1%
29	Submitted to University of Birmingham Student Paper	<1%
30	Submitted to University of Houston System Student Paper	<1%
31	Submitted to University of Pretoria Student Paper	<1%
32	Submitted to University of Western Australia Student Paper	<1%
33	Submitted to Universiti Malaysia Pahang Student Paper	<1%
34	Submitted to British University in Egypt Student Paper	<1%
35	Submitted to University of Oklahoma Student Paper	<1%
36	Submitted to University of Newcastle upon Tyne Student Paper	<1%
37	Submitted to Democritus University Student Paper	<1%
38	Submitted to 2702 Student Paper	<1%
39	Submitted to University College London Student Paper	<1%
40	Submitted to Universiti Putra Malaysia Student Paper	<1%

41

Submitted to Universidad Nacional de Colombia

Student Paper

<1%

42

Submitted to Heriot-Watt University

Student Paper

<1%

43

Submitted to Cardiff University

Student Paper

<1%

Exclude quotes Off

Exclude matches Off

Exclude bibliography Off